Monte Carlo Simulations of the Solution Structure of Simple Alcohols in Water−Acetonitrile Mixtures

Peter I. Nagy* and Paul W. Erhardt

Center for Drug Design and Development, College of Pharmacy, The University of Toledo, Toledo, Ohio 43606-3390

Received: September 29, 2004; In Final Form: January 20, 2005

Monte Carlo simulations have been performed to explore the solution structure of ethyl, isopropyl, isobutyl, and tertiary butyl alcohols in pure water, pure acetonitrile, and different mixtures of the two solvents. The explicit solvent studies in NpT ensembles at $T = 298$ K illustrate that the solute "discriminates" the solvent's components and that the composition of the first solvation shell differs from that of the bulk solution. Since the polarizable continuum dielectric method (PCM) does not presently model the solvation of molecules with both polar and apolar sites in mixed protic solvents, we suggest a direction for further program development wherein a continuum dielectric method would accept more than one solvent and the solute sites would be solvated by user-defined solvent components. The prevailing solvation model will be determined upon the lowest free energy calculated for a particular solvation pattern of the solute having a specific conformational/tautomeric state. Characterization of equilibrium hydrogen-bond formation becomes a complicated problem that depends on the chemical properties of the solute and its conformation, as well as upon the varying nature of the first solvation shell. For example, while the number of hydrogen bonds to secondary and tertiary alcohol solutes are nearly constant in pure water and in water−acetonitrile mixtures with at least 50% water content, the number of hydrogen bonds to primary alcohols gradually decreases for most of their conformations when acetonitrile content is increased. Nonetheless, the calculations indicate that $O-H\cdots O_{water}$ hydrogen bonds are still possible in a small fraction of the arrangements for the solution models with water content of 30% or less. The isopentene solute does not form any observable hydrogen bonds, despite having an electron-rich, double-bond site.

Introduction

Most laboratory reactions are conducted in solution where it is well-known that the solvent can often have a significant effect on reaction rate and, in some cases, can also dictate the type of product that is formed. Thus, quantum chemical characterization of the isolated (gas-phase) reactants is not adequate in such cases, particularly when delineations of the reaction route and the transition state are being sought.

Characterization of solvent effects at the ab initio[1] or DFT[2] quantum chemical levels is possible by applying continuum dielectric solvent models.[3] Although there are different implementations, the common approach in these methods is that the solvent environment is represented by a homogeneous and polarizable dielectric characterized by its dielectric constant at a given temperature. The solute is placed in a cavity carved in the dielectric. Different methods use different techniques for defining the cavity, but all calculations then continue with the solution of the Schrodinger equation for a solute immersed in a dielectric. The solute polarizes the dielectric such that image charges are induced on the cavity surface. A reaction potential operator, V_R, can be established on the basis of the created image charges, and an SCF procedure is used to find the converged image charges and subsequently the converged form of the V_R operator. The E^s_{int} internal energy of the solute in solution, as well as the E_{susv} solute−solvent interaction energies are then calculated as follows:

$$E^s_{int} = [\langle \Psi_s | H^\circ | \Psi_s \rangle] \quad (1a)$$

$$E_{susv} = [\langle \Psi_s | V_R{}^{sol} | \Psi_s \rangle] \quad (1b)$$

wherein H° is the solute Hamiltonian, $V_R{}^{sol}$ is the solvent reaction potential (frequently called the "reaction field") generated by the fully polarized solute in solution, and Ψ_s is the converged wave function of the solute.

In conjunction with synthetic studies being conducted in our laboratories, we sought to address the problem of how to best account for solvent effects when using a continuum dielectric model for the reaction of a secondary alcohol in a mixed solvent, namely, in a water−acetonitrile mixture. Dielectric constants for mixtures of water and acetonitrile are known from experiment.[4] The question was raised, however, whether the bulk dielectric constant properly characterizes the chemical environment in the first solvation shell of the alcohol group. Although remote interactions may also be important, the closest solvent molecules certainly play the most significant roles throughout the reaction path as well as across the transition state. Thus, the immediate question was whether a polar group like an alcoholic OH might prefer to selectively associate with one of the more polar, hydrogen-bonding solvent components such that the local concentration of that component would then differ from its calculated concentration in the bulk solvent. To address this question, a variety of simple alcohols were deployed as probes to assess the influence of a solute's steric and electronic effects upon its potentially selective interactions at infinite dilution with

* Corresponding author: e-mail pnagy@utnet.utoledo.edu.

10.1021/jp045570q CCC: $30.25
Published on Web 03/08/2005

SCHEME 1: Newman Projections for the Studied Conformers[a]

A

B

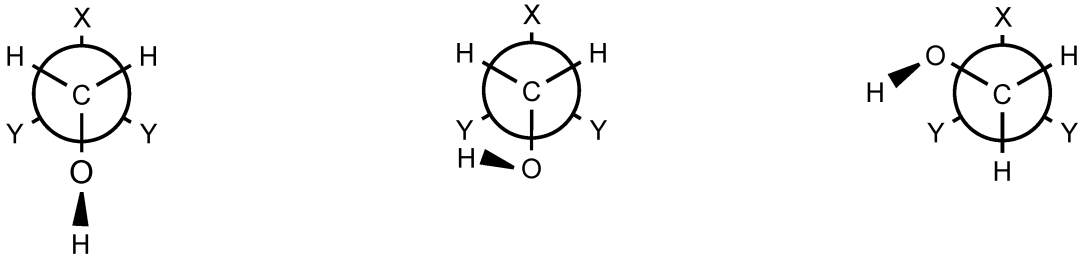

[a] Lone pairs for the oxygens are not indicated. (A) For EtOH (both conformations studied), X = CH_3 and Y = H; for *i*-PrOH (both conformations studied), X = H and Y = CH_3; for *t*-BuOH (one conformation studied since trans = gauche), X = Y = CH_3. (B) For *i*-BuOH, X = H and Y = CH_3. All conformers were studied in pure water, pure acetonitrile, and water−acetonitrile mixtures with compositions of 50:50 and 30:70.

one or the other components of a simple binary solvent system having varying ratios. The solutes' conformations were also taken into consideration as a prelude to examining an explicit model for each ratio of solvents.

Monte Carlo (MC) simulations have been carried out for conformers of ethanol (EtOH), isopropyl (*i*-PrOH), isobutyl (*i*-BuOH), and tertiary butyl (*t*-BuOH) alcohols in pure solvents and in water−acetonitrile mixtures of different compositions. We also performed simulations for an isopentene (3-methylbut-1-ene) structure to additionally probe the sensitivity of the structure prediction from our method. The results were analyzed by interpreting the solute−solvent interaction energies and the radial distribution and pair-energy distribution functions for the solutes in different solutions.

The present MC studies consider the solutes as rigid systems with selected conformations (Scheme 1). Although this restriction need not be imposed when a molecular dynamics approach is taken, such an approximation was in line with our future goals where a reaction potential energy surface (PES) is to be calculated for a specified alcohol reactant. In a recently proposed in-solution structure analysis procedure,[5a−c] the internal energy of the solute is to be calculated at different points of the PES with a given conformation by means of a continuum solvent approach, and the relative solvation free energy along the transformation path is to be calculated with the free energy perturbation method, as implemented in MC simulations.[6] Thus, the present approach is well-suited for future calculations to be performed on reactions of alcohols in water−acetonitrile mixtures.

Methods and Calculations

Geometric Aspects of the Conformations. A given alcohol can form hydrogen bonds as either a donor, an acceptor, or both. Previous MC simulations for 1,2-ethanediol[7] in aqueous solution have clearly shown that hydration of the trans CCOH moiety is superior to that of the gauche structure. The O−H···O_w hydrogen bond (favorably available only in the trans conformation) is more stable than the O···H_w−O_w hydrogen bond in either the gauche or the trans conformation (the w subscript refers to the water atom). As noted above, each solute resides in a single conformation throughout the simulations undertaken in the present study, and only all-staggered arrangements about rotatable bonds have been considered.

A single staggered conformation exists for *t*-BuOH due to a 3-fold potential for the rotation of the alcoholic hydrogen about the O−C bond. Rotational spectra of EtOH have been interpreted that this alcohol takes both the CCOH trans and gauche conformations in the gas phase.[8] Accordingly, both conformations have been studied in solution, as well. For *i*-PrOH, there are two stable conformations corresponding to trans and gauche HCOH arrangements. Solvation of both conformers have been investigated.

i-BuOH can exist in a mixture of staggered conformers. One of them has a symmetry plane by adopting trans conformations for both the HCCO and the CCOH moieties. By assigning the HCCO conformations as T(rans) or G(auche) and the CCOH arrangements as t(rans) of g(auche), the structure will be referred henceforth to as the Tt conformation. If only staggered conformations are considered, there are 3 × 3 conformers derived from independent rotations by 120° about each of the −CH−CH_2 and the C−O bonds. Eight of the resulting nine structures form four pairs of mirror-image structures, whereas Tt is a unique conformation with C_s symmetry. Although no complete conformational analysis has been performed for *i*-BuOH in the gas phase and in solution, two further structures were studied, as well. Study of the Tg conformer in comparison with the Tt form allows exploration of the effect when the alcoholic hydrogen rotates from the CCOH trans to gauche position. Such an XCOH rotation has been considered also for EtOH and *i*-PrOH. Consideration of the Gt form for *i*-BuOH

helps assess the importance of the HCCO rotation throughout solvation. The CCOH conformation was selected as trans in this case for ensuring the largest exposure of the alcoholic hydrogen to solvation. In the case of a Gg^+ or Gg^- conformation (CCOH would be a sort of gauche) the close methyl group(s) could sterically hinder the solvation of the alcoholic hydrogen.

Serving as a proton donor, an alcoholic group can also form an intermolecular hydrogen bond with acetonitrile, and in this case, consideration of the XCOH arrangement is even more critical. Acetonitrile has a linear N−C−C skeleton. Formation of the O−H···N hydrogen bond is always energetically accessible for an alcohol in a trans XCOH arrangement. For a gauche XCOH arrangement, steric repulsion may become prohibitive for solutes having bulky groups, that is, a gauche arrangement of the isopropyl group in *i*-BuOH.

Conformational Equilibria. Consideration of different molecular structures in solution provides information about the solvation of specific conformers. It remains unclear, however, what fraction a given conformer takes in the equilibrium mixture. The equilibrium constant, K, for two species is related to their standard free energy difference, $\Delta G°$, at the T temperature as $\Delta G° = -RT \ln K$. $\Delta G°$ can be routinely calculated for pure ideal-gas conformers at T and p pressure of 1 bar as[9,10]

$$\Delta G_g^{\,o} = \Delta E(\text{int}) + \Delta\text{ZPE} + \Delta[H_{\text{vibr}}(T) - \text{ZPE}] - T\Delta S(T) - RT\,\Delta\ln(\sigma) \quad (2)$$

Subscript g refers to gas-phase terms, and all terms in eq 2 are to be calculated for the gas phase. ΔE(int) is the quantum chemically calculated internal molecular energy difference for the conformers obtained after geometry optimization. ΔZPE is the difference of the zero-point vibrational energy. $H_{\text{vibr}}(T)$ and $S(T)$ stand for the vibrational energy and the total entropy for the molecule at T, respectively. σ is related to the symmetry of the species and its values are 2 and 1 for structures without and with a mirror plane, respectively. The $-RT \ln \sigma$ term with $\sigma = 2$ accounts for the free energy contribution due to the entropy of mixing for mirror image pairs. In eq 2, the $\Delta[E_{\text{trans}} + E_{\text{rot}} + pV(T)]$ term [where $V(T)$ is the molar volume at T] does not appear because the sum is constant, $4RT$/mol for molecules (with at least three nonlinear atoms). By use of the rigid rotor−harmonic oscillator approximation[10] for the conformers, the Gaussian 98 software[11] calculates the values of the individual terms in eq 2.

Calculation of the standard free energy difference for two conformers, $\Delta G_s^{\,o}$ in solution (subscript s refers to in-solution terms) requires more terms:

$$\Delta G_s^{\,o} = \Delta E(\text{int}) + \Delta G(\text{solv}) + \Delta\text{ZPE} + \Delta[H_{\text{vibr}}(T) - \text{ZPE}] - T\Delta S_{\text{vibr}}(T) - RT\,\Delta\ln(\sigma) + \Delta[E_{\text{trans}}(T) + E_{\text{rot}}(T) - TS_{\text{trans}}(T) - TS_{\text{rot}}(T) + pV(T)] \quad (3a)$$

The most important new term in eq 3a as compared to eq 2 is the ΔG(solv) term standing for the relative solvation free energy. By use of the PCM method,[3b,c] $\Delta G(\text{solv}) = {}^1/_2\Delta E_{\text{susv}} + \Delta G_{\text{drc}}$. ΔE_{susv} is to be calculated from eq 1b, and ΔG_{drc} stands for the nonelectrostatic relative dispersion-repulsion-cavity term. The PCM method as implemented in the Gaussian 98 software[11] provides the terms for ΔG(solv).

The $\Delta[E_{\text{trans}}(T) + E_{\text{rot}}(T) - TS_{\text{trans}}(T) - TS_{\text{rot}}(T) + pV(T)] = \Delta G\text{corr(ection)}$ term at $T = 298$ K was neglected in the present application. There is no solid theoretical method to calculate the involved energy and entropy components for solute molecules in solution. As was discussed in several previous papers,[5] the ΔGcorr value above may be remarkable for molecules of different chemical compositions or in cases when the molecule moves from one phase into another, for example, at solvation of a gas-phase molecule. The above term should be, however, close to zero for slightly different conformers of a solute in the same solvent. The volume work, $pV(T)$, also differs very little for conformers of small molecules, as revealed from Monte Carlo studies (see below).

The vibrational frequency-dependent correction, $\Delta\text{ZPE} + \Delta[H_{\text{vibr}}(T) - \text{ZPE}] - T\Delta S_{\text{vibr}}(T)$, calculated in the rigid rotor−harmonic oscillator approximation is an even less adequate approach for solutes than for gas-phase molecules. Furthermore, a real solvent does not establish equilibrium conditions around the solute within a period of a vibration. For similar molecules, like conformers, however, the *difference* of the frequency-dependent correction terms may have relevance under similar conditions for them in the solution.

The standard free energy for a solute refers to a hypothetical state to be calculated at a concentration of 1 mol/dm^3. By use of the PCM continuum dielectric or the Monte Carlo explicit-solvent solvation models, the calculated ΔG(solv) values are good approximations to the solvation part of the relative standard free energies of solutes.[5a,b]

Overall, the relative free energy in solution can be approximated as

$$\Delta G_s^{\,o} = \Delta E(\text{int}) + \Delta G(\text{solv}) + \Delta\text{ZPE} + \Delta[H_{\text{vibr}}(T) - \text{ZPE}] - T\Delta S_{\text{vibr}}(T) - RT\,\Delta\ln(\sigma) \quad (3b)$$

Molecular structures were optimized by using the Gaussian 98 software running on a Cray SV1ex supercomputer at the Ohio Supercomputer Center. Gas-phase optimizations were performed at the B3LYP/6-31G* level.[1,2] The polarizable continuum method (PCM)[3b,c] method, as implemented in Gaussian 98, was applied for geometry optimization in pure water and acetonitrile. The in-solution geometry optimizations were performed at the B3LYP/6-31G* level with the default icomp = 2 parametrization. Dielectric constants of $\epsilon = 78.39$ and 35.84 were accepted for water and acetonitrile, mimicking solvents at $T = 298$ K.[12] Local-energy-minimum characters of the conformers were certified by frequency analyses both in the gas phase and in solution. Geometric parameters for the C−O−H moiety are provided in Table 1. For the *trans*-isopropyl alcohol, each of the *i*-PrOH−water and *i*-PrOH−acetonitrile dimers was optimized in both pure solvents, and local energy minimum characters were certified by all nonnegative eigenvalues for the second-derivative matrixes.

The final wave function was obtained from a single-point calculation at the optimized geometry with the icomp = 4 parameter setting.[5a] By using the icomp = 4 instead of 2 parameter value in PCM calculations, care is taken for the escaped charge in a more sophisticated way than with the default value, and this larger precision is important in the derivation of the atomic charge parameters for MC simulations. B3LYP/6-311++G**//B3LYP/6-31G* single-point calculations for studying the basis set effect on the conformational energy and derived atomic charges were performed in the gas phase and in acetonitrile and water solvents.

Charge Derivation. Atomic charges for MC simulations (Tables 2 and 3) were derived by fitting the PCM/B3LYP wave function to the in-solution molecular electrostatic potential (ELPO)[5a−c] by means of the CHELPG procedure.[13] In every case, the corresponding B3LYP/6-31G* optimized geometry and the B3LYP/6-31G* and the single-point B3LYP/6-311++G**//

TABLE 1: B3LYP/6-31G* Optimized Geometric Parameters for the C−O−H Site of Alcohols in the Gas Phase and in Acetonitrile and Water Solvents[a]

	gas			acetonitrile[b]			water[b]		
MeOH									
C−O		1.419 (1.425)[c]			1.421			1.424	
O−H		0.969 (0.945)			0.971			0.979	
COH		107.7 (108.5)			107.4			107.2	
EtOH[d]	gauche	trans		gauche	trans		gauche	trans	
C−O	1.424	1.425		1.427	1.427		1.430	1.430	
O−H	0.970	0.969		0.973	0.972		0.982	0.979	
COH	107.4	107.9		107.1	107.7		106.2	107.5	
PrOH[d]		trans			trans			trans	
C−O		1.424			1.426			1.429	
O−H		0.969			0.972			0.979	
COH		107.9			107.7			107.2	
i-BuOH[e]	Tt	Tg	Gt	Tt	Tg	Gt	Tt	Tg	Gt
C−O	1.426	1.425	1.425	1.427	1.429	1.427	1.431	1.432	1.429
O−H	0.968	0.969	0.969	0.972	0.971	0.972	0.980	0.982	0.981
COH	107.9	107.6	107.9	107.5	107.8	107.7	107.3	108.0	107.4
i-PrOH[f]	gauche	trans		gauche	trans		gauche	trans	
C−O	1.431	1.430		1.434	1.434		1.436	1.436	
O−H	0.970	0.971		0.973	0.974		0.982	0.983	
COH	107.6	107.1		107.2	106.9		106.4	107.1	
t-BuOH									
C−O		1.439			1.441			1.442	
O−H		0.971			0.973			0.982	
COH		107.3			107.1			107.4	

[a] Distances are given in angstroms; angles are given in degrees. [b] PCM/B3LYP/6-31G* optimizations at $T = 298$ K; $\epsilon = 35.84$ and 78.39 for acetonitrile and water, respectively. [c] Experimental values are given in parentheses; ref 19. [d] CCOH gauche and trans structures. [e] For letter codes T,G, t, and g see the text. [f] HCOH gauche and trans structures.

B3LYP/6-31G* wave functions were utilized. For gas-phase charge derivations the corresponding gas-phase counterparts (geometry, wave function, and basis sets) were utilized.

Derivation of in-solution atomic charges relevant for water−acetonitrile mixtures was attempted for *n*-propyl alcohol. In the present implementation of PCM in Gaussian 98, one has to choose a solvent (water or acetonitrile in our case) as an input SCRF parameter. Upon choosing the water solvent and setting the dielectric constant to the corresponding value measured for a water−acetonitrile mixture,[4] we expected a derived charge set representing the mixture. Although the modified dielectric constants were accepted by the system, the derived charges hardly changed from pure water to the mimicked composition of water:acetonitrile = 2:8 (molar ratio). Starting from the acetonitrile side (the parameter for the solvent name is "acetonitrile") resulted in values almost identical with those obtained with pure acetonitrile, even with a composition of water:acetonitrile = 6:4. The likely reason for the small changes in the derived charge parameters is that although the program modifies the dielectric constant within the range of 78.4 and 35.8, the cavity parameters remain unchanged as defined by the solvent name. For example, the so-called α parameter is 1.20 for water and 1.40 for acetonitrile. As testified by the output, these values did not change even when the dielectric constant mimicked a mixture. Indeed, the system cannot change this parameter to an intermediate value, because only one solvent name is provided, and the present implementation does not allow naming two solvents. Table 2 shows, however, that the charges derived with each of the pure solvents change only a little. In the end, we used the water-based charges from Table 2 for mixtures with at least $x = 0.5$ (molar ratio) water, while the acetonitrile-based parameters were used for simulations with x (acetonitrile) > 0.5. For a discussion of charges in Table 3, see the Results section.

Monte Carlo Simulations. MC simulations[14] were performed with the BOSS 3.6 program[15a] in NpT (isothermal−isobaric) ensembles at $T = 298$ K and $p = 1$ atm. A box of 508 TIP4P water molecules[16] and a box of 263 acetonitrile molecules surrounding a single solvent molecule were used for simulations with pure solvents. The three-point (united methyl-atom) model of Jorgensen and Briggs[17] was used for the acetonitrile solvent. Different water−acetonitrile compositions were obtained by replacing the primary solvent molecules with a number of molecules of the secondary solvent (Table 6). These solution models correspond to infinitely dilute solutions. A recent study showed that this model does not result in a serious error up to a concentration of about 1 M.[5b]

Interaction energies of the solution elements were calculated by using the all-atom OPLS 12-6-1-AA pair-potential.[18] In this model, all solute atoms are considered explicitly whereas the four and three center models for the TIP4P and MeCN solvent models, respectively, are still maintained. Geometries for the solute conformers were obtained from PCM/B3LYP/6-31G* geometry optimizations in water and acetonitrile. The intramolecular geometric parameters were kept rigid throughout calculations of the interaction energies between any two molecules in the solutions.

Steric OPLS parameters were taken from ref 18. Atomic charges were derived as described above. Charges, experimental and quantum chemical dipole moments, and dipole moments calculated from the ELPO atomic charges are compared in Table 2. For the maximum considered solute−solvent and the solvent−solvent interactions, SCUT = 12 Å and RCUT = 9.75 Å cutoffs were accepted, respectively. By utilization of the ICUT = 2 option in BOSS 3.6, every solvent molecule is seen by the solute if the central atom of the solvent is within a sphere of SCUT around any solute atoms. Random translation and rotation for the solute were limited to 0.1 Å and 10°, respectively. A solute move was attempted in every 50 steps. Volume alteration (with a maximum of 600 Å^3) was attempted in every 1000 steps. Periodic boundary conditions and preferential sampling were applied with the a value of 120 Å^2 for the adjustable c constant

in the sampling factor $1/(R^2 + c)$, where R is the distance between a specified atom of the solute and the central atom of the selected solvent molecule. With these simulation parameters, 40−60% of the newly generated configurations were accepted.

In pure solvents with preequilibrated solvent boxes, 5000K (5 000 000) configurations were considered in the equilibration phase, and data were collected from the subsequent 7500K configurations. In mixtures, at least 26000K configurations were considered in the equilibration phase, and data were collected from the subsequent 7500K configurations. The long equilibration phase was necessary to reduce the probability of a poorly equilibrated solution structure. Replacements of solvent molecules in an equilibrated box with entirely different molecules of another solvent, that is, water with acetonitrile and vice versa, generally lead to large increases in the total energy of the system. Since the replacement of *n*2 solvent1 molecules with *n*2 solvent2 molecules took place randomly, the starting local concentrations nearly reflected the bulk composition with a preset composition of $N(\text{total}) = n1(\text{solvent1}) + n2(\text{solvent2})$. After 5000−10000K configurations were considered for mixtures, however, the solvent molecules generally started to form islands or chains of the water and/or the acetonitrile molecules. Only long equilibration phases and relatively small standard deviations for some thermodynamic parameters can be used to ascertain that the system has been equilibrated. The BOSS program obtains the final value and standard deviation for a thermodynamic quantity by averaging subaverages calculated in consecutive steps. A step means consideration of a predefined number of configurations, 100K in the present case. In the averaging phase of our study, 75 steps were made and the jobs were run interactively for all mixtures. The energy output was regularly checked after 300−500K configurations. On the basis of the Cartesian coordinates for the solution elements at the end of the steps, the solution structure was regularly inspected by utilizing the graphical display capacity of a Silicon Graphics workstation. Even after altogether about 33000K configurations were considered, surprising structural changes were noticed and required further consideration of an additional 5000K configurations for *t*-BuOH in water:acetonitrile = 10:90 mixtures (see the Results section).

Discussion of the solution structure is based on a combined analysis of the calculated, OPLS-optimized interaction energies of the alcohol−water and alcohol−acetonitrile dimers in the gas phase (Table 5), the solute−solvent interaction energies in solution (Table 6, Figures 1−3), the radial distribution functions in pure solvents (Figures 4−6), and the pair-energy distribution functions (Figures 7−15).

Results and Discussion

Geometries and Atomic Charge Parameters. B3LYP/6-31G* optimizations provide good geometries for small neutral molecules such as methylamine, aniline, and phenol.[5c] The calculated C−O−H geometric parameters for methanol in gas phase (Table 1) are also in good agreement with experimental results.[19] Although the microwave spectra for both the gauche[8a] and trans[8b,c] conformers of EtOH were obtained, no molecular structures were provided in those studies. B3LYP/6-31G* geometry optimizations show that the corresponding differences in the C−O and O−H bond lengths for the conformers are negligible in a given chemical environment. The COH bond angle changes by up to 1°, but no clear trend has been observed. For example, this angle is larger in the case of the trans than the gauche conformer for EtOH both in the gas phase and when it is solvated with acetonitrile, whereas the opposite was found for the *i*-PrOH molecule.

In the case of a given conformer, the bond lengths increase upon solvation and with the solvent polarity. The increase is no more than 0.007 Å for the C−O bond length but is more than 0.01 Å for the otherwise shorter O−H bond. Change of the COH angle is not monotonic. It decreases with the solvent polarity for primary alcohols but shows a small minimum in acetonitrile for the Tg conformer of *i*-BuOH, the trans conformer of *i*-PrOH, and *t*-BuOH. The change in the COH angle is the largest for the gauche conformer of EtOH and *i*-PrOH, namely, 1.2° for each in aqueous solution compared to the gas-phase values.

Calculated atomic charges are compared in Tables 2 and 3. Two basis sets were applied in the charge derivation, while the corresponding B3LYP/6-31G* optimized geometry was used consistently. The solvent effect, mainly the effect of the aqueous environment relative to the gas phase, increased the atomic charges by about 10% (in absolute value) when the 6-31G* basis set was used. The increase in atomic charges reached 15−20% in some cases with the 6-311++G** basis set. Calculated free energies of hydration for small molecules depend sensitively on the accepted atomic charge set.[5b] Thus, it became a major question in the present application whether the B3LYP/6-31G* or the B3LYP/6-311++G**//B3LYP/6-31G* wave function is more appropriate for fitting the charges to the molecular electrostatic potential in the gas phase and in solution (from PCM calculations).

Experimental dipole moments available for the gas-phase molecules may serve as a guide for the basis-set selection (Table 2). The B3LYP/6-31G* gas-phase dipole moments are in excellent agreement with the experimental values for MeOH and gauche EtOH. In both cases the B3LYP/6-311++G**//B3LYP/6-31G* value is overestimated by about 10%. In all other cases, the B3LYP/6-311++G**//B3LYP/6-31G* dipole moment is higher by about 7−15% than the corresponding gas-phase B3LYP/6-31G* value, whereas the latter values are closer to the experimental values in most cases than their B3LYP/6-311++G** counterparts.

On the basis of the above analysis, the PCM/B3LYP/6-31G* wave function was utilized for deriving charges for in-solution calculations. Table 2 shows that even the acetonitrile solvent with dielectric constant of 35.84 noticeably polarizes the simple alcohols. All calculated atomic charges increase (in absolute value) going from the gas phase to the acetonitrile and aqueous solution. Dipole moments calculated with the ELPO fitted atomic charges (see the values in parentheses) are in close agreement with the quantum chemically calculated values, the deviations being up to 0.06 D. Such close agreement is a necessary condition for the correct representation of the in-solution charge distribution, although the accord in dipole moments still does not guarantee the quality of the derived charges.

It is striking how different the C atomic charges are for different alcohols. This deviation is not a consequence of the solvent effects because the C atom connecting to the oxygen deviates even in the gas phase by 0.54 unit for the Tt *i*-BuOH conformer and *t*-BuOH. The large deviations illustrate the importance of the number of connecting alkyl groups. *t*-BuOH, with a tertiary central carbon, can be much more polarized than *i*-BuOH with a primary carbon. This large polarization difference holds only for the C atom. Atomic charges in the connected OH group change only moderately.

The atomic charges for the O-connected carbon atoms differ even for the primary alcohols. The charges do not change monotonically with an increase in aliphatic chain length. For

TABLE 2: Derived C−O−H Atomic Charges from B3LYP/6-31G* and B3LYP/6-311++G//B3LYP/6-31G* Calculations for Alcohols in the Gas Phase and from the Corresponding PCM Calculations in Acetonitrile and Water Solvents**

	gas		acetonitrile[a]		water[a]	
	6-31G*	6-311++G**	6-31G*	6-311++G**	6-31G*	6-311++G**
			MeOH			
C	0.220	0.319	0.227	0.339	0.227	0.349
O	−0.608	−0.668	−0.646	−0.722	−0.674	−0.759
H	0.391	0.404	0.417	0.437	0.439	0.462
DM[b]	1.695	1.887	1.893	2.145	2.038	2.287
	(1.677)	(1.841)	(1.874)	(2.090)	(2.018)	(2.230)
DM_{exp}[c]		1.70 ± 0.02				
			EtOH gauche[d]			
C	0.383	0.464	0.401	0.496	0.410	0.508
O	−0.642	−0.699	−0.683	−0.761	−0.712	−0.807
H	0.387	0.397	0.415	0.433	0.436	0.465
DM	1.674	1.870	1.910	2.200	2.112	2.460
	(1.667)	(1.833)	(1.901)	(2.152)	(2.107)	(2.413)
DM_{exp}[c]		1.68 ± 0.03				
			EtOH trans[d]			
C	0.397	0.484	0.404	0.500	0.407	0.503
O	−0.635	−0.700	−0.671	−0.757	−0.703	−0.805
H	0.380	0.394	0.406	0.429	0.429	0.463
DM	1.563	1.756	1.805	2.085	1.981	2.290
	(1.533)	(1.699)	(1.774)	(2.018)	(1.948)	(2.218)
DM_{exp}[c]		1.44 ± 0.03				
			PrOH trans[d]			
C	0.275	0.349	0.284	0.372	0.285	0.380
O	−0.662	−0.726	−0.698	−0.782	−0.728	−0.825
H	0.405	0.419	0.431	0.456	0.453	0.493
DM	1.489	1.638	1.741	1.972	1.912	2.171
	(1.498)	(1.629)	(1.745)	(1.951)	(1.916)	(2.149)
DM_{exp}[c]		1.55 ± 0.03				
			i-BuOH Tt[e]			
C	0.136	0.179	0.152	0.207	0.154	0.215
O	−0.632	−0.674	−0.661	−0.720	−0.695	−0.767
H	0.410	0.412	0.432	0.443	0.456	0.474
DM	1.516	1.629	1.760	2.034	2.020	2.455
	(1.493)	(1.585)	(1.737)	(1.981)	(1.993)	(2.393)
			i-BuOH Tg[e]			
C	0.188	0.242	0.190	0.253	0.192	0.261
O	−0.600	−0.647	−0.632	−0.697	−0.666	−0.742
H	0.381	0.385	0.402	0.414	0.427	0.446
DM	1.637	1.816	1.873	2.147	2.037	2.359
	(1.623)	(1.772)	(1.855)	(2.090)	(2.016)	(2.300)
DM_{exp}[c]		1.64 ± 0.08				
			i-BuOH Gt[e]			
C	0.176	0.227	0.208	0.276	0.193	0.265
O	−0.648	−0.700	−0.686	−0.755	−0.712	−0.788
H	0.409	0.416	0.434	0.451	0.457	0.481
DM	1.448	1.538	1.702	1.832	1.886	1.963
	(1.449)	(1.529)	(1.700)	(1.813)	(1.884)	(1.943)
			i-PrOH gauche[f]			
C	0.543	0.631	0.565	0.671	0.576	0.704
O	−0.662	−0.725	−0.704	−0.791	−0.735	−0.836
H	0.383	0.393	0.409	0.431	0.431	0.463
DM	1.559	1.763	1.839	2.122	2.041	2.222
	(1.552)	(1.733)	(1.830)	(2.083)	(2.029)	(2.181)
			i-PrOH trans[f]			
C	0.506	0.598	0.534	0.635	0.562	0.669
O	−0.655	−0.713	−0.696	−0.774	−0.734	−0.835
H	0.380	0.388	0.409	0.425	0.432	0.460
DM	1.615	1.819	1.874	2.125	1.993	2.420
	(1.638)	(1.812)	(1.894)	(2.115)	(2.014)	(2.405)
DM_{exp}[c]		1.58 ± 0.03				
			t-BuOH			
C	0.673	0.779	0.695	0.820	0.715	0.854
O	−0.688	−0.757	−0.725	−0.816	−0.756	−0.854
H	0.382	0.390	0.406	0.425	0.426	0.452
DM	1.511	1.732	1.809	2.082	1.946	2.081
	(1.523)	(1.724)	(1.819)	(2.065)	(1.955)	(2.067)
DM_{exp}[c]		1.66				

[a] Optimized geometries and wave functions from PCM/B3LYP calculations. [b] Dipole moments (DM) are given in debyes. Values in parentheses are from the CHELPG/ELPO fit. [c] Reference 12. [d] CCOH gauche and trans structures. [e] For T, G, t, and g codes, see the text. [f] HCOH gauche and trans structures.

TABLE 3: Intermolecular Geometric Data and Derived C−O−H Atomic Charge Parameters for the trans *i*-PrOH−OH_2 and *i*-PrOH−NCMe Dimers from B3LYP/6-31G* Calculations[a]

	i-PrOH−OH_2	*i*-PrOH−NCMe
	Gas	
H···X	1.94	2.12
O−H···X	155	180
q(C, O, H)	0.602, −0.723, 0.392	0.574, −0.706, 0.416
q(tot)	−0.040	−0.031
	Acetonitrile	
H···X	1.87	2.04
O−H···X	179	177
q(C, O, H)	0.637, −0.773, 0.433	0.554, −0.733, 0.425
q(tot)	−0.040	−0.039
	Water	
H···X	1.86	2.05
O−H···X	170	172
q(C, O, H)	0.617, −0.797, 0.442	0.540, −0.748, 0.423
q(tot)	−0.047	−0.040

[a] Calculations were for the gas phase and for pure acetonitrile and water solvents. Distances are given in angstroms; angles are given in degrees. The *q*(tot) charge indicates the net charge on *i*-PrOH due to the charge transfer from the acetonitrile and water hydrogen-bond acceptor molecules.

example, the gas-phase atomic charge for the trans EtOH conformer (0.397) is larger than that for MeOH (0.220) and the trans PrOH conformer (0.275). The primary carbon in the branched-chain *i*-BuOH bears the smallest charge: 0.136 unit for the Tt conformer. It is important to remark that the C, O, and H atomic charges show only small dependence on the conformation of the species, but all of them consistently increase in absolute value going from the gas phase to solution with increasing solvent polarity.

The solvent effect does not modify the trend found for the charge of the O-connected C atom in the gas-phase structures. The values slightly increase, but the differences hardly change. The O atomic charges are in the range of −0.60 to −0.69 for the gas-phase alcohols. The ranges are −0.65 to −0.73 and −0.67 to −0.76 in acetonitrile and in water, respectively. The three respective ranges for the alcoholic hydrogens are 0.38−0.41, 0.41−0.43, and 0.43−0.46. The large deviations for the primary carbon atoms, and the still remarkable departures for the alcoholic oxygens, suggest that separate charge parametrizations are necessary for different molecules. Neighboring polar groups or those that can form intramolecular hydrogen bonds must have an important influence on the resulting charges,[7,20] but even connecting methyl groups may cause considerable modifications.

Table 3 summarizes the results for the optimized *i*-PrOH−OH_2 and *i*-PrOH−NCMe dimers in the gas phase and in acetonitrile and aqueous solutions. By this supermolecule/continuum approach we intended to consider the polarization of the alcohols upon hydrogen-bond formation in different solvents. The optimized H···X (X = O, N) distances in the condensed phase are close to the maxima of the MC radial distribution functions (see the Structure of the First Solvation Shell section). Thus, the PCM/B3LYP/6-31G* optimized geometries are in fortuitous agreement with the average H···X separations from MC simulations, where the thermal disordering effects are also considered. On this basis, ELPO fitted atomic charges in Table 3 could be a better approximation for the net atomic charges than those summarized in Table 2.

There are, however, three problems with the charges in Table 3. The most serious is that upon hydrogen-bond formation there is a charge transfer from the acceptor molecules to *i*-PrOH. The solute must be neutral during MC simulations in the present application; thus the *q*(tot) charges have to be removed from *i*-PrOH. There is no sound, theoretical recipe for this charge removal. A tempting, although not justified, procedure is to reduce the alcoholic oxygen charges by *q*(tot). In that case, the *i*-PrOH atomic charges in Tables 2 and 3 get closer, even though the values in Table 3 still predict a more polarized alcoholic structure.

By consideration of discrete solute−solvent pairs, two slightly different sets have been obtained for the C−O−H charges in the two solvents, depending on whether the charges were deduced by means of the wave function for the *i*-PrOH−OH_2 or the *i*-PrOH−NCMe dimer. The BOSS 3.6 program accepts a single charge set for the solute in a given solvent. In the mixed solvents, where both types of hydrogen bonds are possible, an approximation may be to take the averages of all derived charges. The third problem is that the supermolecule/continuum approach optimizes the geometry by minimizing the dimer energy in the continuum solvent. Thus, the derived geometric and charge parameters reflect the energetically most favorable interactions for the elements in the dimer. Thermal disordering acts in the opposite direction, thus the average interaction during MC simulations would not be as strong as from that for energy-minimized structures. Consequently, charges in Table 3 do not reflect the parameters of the average solute−solvent interaction in MC simulations. If one reduces the oxygen atomic charges by *q*(tot), takes the averages of the corresponding charges in Table 3, and considers that the obtained values refer to energy-minimized and not average interactions, then the values will be close to those in Table 2, which may provide an acceptable charge set for simulations.

Conformational Analysis. Relative energies and thermal corrections are summarized for two EtOH, two *i*-PrOH, and three *i*-BuOH conformers in Table 4. All geometries were optimized at the B3LYP/6-31G* level. The relative energies differ sometimes even in their sign from B3LYP/6-31G* and B3LYP/6-311++G**//B3LYP/6-31G* single-point calculations. The conformational energy differences, however, are small in every case, not exceeding 0.5 kcal/mol.

For EtOH, the gauche conformer is more stable than the trans form in all three chemical environments. The 6-311++G** basis set finds the trans form more stable than the gauche by 0.06 kcal/mol in the gas phase. For this pair, not only are the individual dipole moments known from experiment, 1.68 ± 0.03 and 1.44 ± 0.03 D for the gauche and trans conformer, respectively (Table 2), but the dipole moment for the gas-phase equilibrium mixture is available as well. The average experimental dipole for EtOH is 1.69 ± 0.3 D.[12] By assuming that the contribution of the two conformers in the mixture is simply proportional to their equilibrium fraction, the average cannot be larger than the gauche value of 1.68 ± 0.03 D. Thus, the average value should be taken close to its lower limit, about 1.66 D. Assuming 1.68 and 1.44 D dipole moments for the two conformers, the mixture would consist of 92% gauche and 8% trans conformers. For calculating the theoretical composition, free energies including thermal corrections are to be considered (eq 2). The $\Delta G_{th}(T)$ term in Table 4 includes all but the ΔE term from eq 2, thus the relative free energy can be calculated from these data as $\Delta G_g^o = \Delta E + \Delta G_{th}(T)$. Results with the 6-31G* basis set predict gauche and trans EtOH fractions of 74% and 26%, respectively, at T = 298 K, whereas the corresponding fractions are 61% and 39% with the 6-311++G** basis set. Thus, calculations with the 6-31G* basis set predict

TABLE 4: Relative Energies and Thermal Corrections at $T = 310$ for EtOH, *i*-PrOH, and *i*-BuOH Conformers in the Gas Phase and in Solution from B3LYP and PCM/B3LYP calculations[a]

	gas		acetonitrile		water	
	6-31G* [b]	6-311++G** [c]	6-31G* [d]	6-311++G** [e]	6-31G* [d]	6-311++ G** [e]
EtOH						
trans[f]	0.00	0.00	0.00	0.00	0.00	0.00
gauche	−0.31	0.06	−0.40	−0.04	−0.48	−0.41
i-PrOH						
trans[g]	0.00	0.00	0.00	0.00	0.00	0.00
gauche	0.08	−0.22	0.11	−0.28	0.17	0.37
i-BuOH						
Tt[h]	0.00	0.00	0.00	0.00	0.00	0.00
Tg	−0.46	0.06	−0.38	0.18	−0.29	0.40
Gt	−0.34	−0.48	−0.46	−0.50	−0.36	−0.34

	gas			acetonitrile			water		
	$\Delta H(T)$	$-T\Delta S(T)$	$\Delta G_{th}(T)$[i]	$\Delta H(T)$	$-T\Delta S(T)$	$\Delta G_{th}(T)$[i]	$\Delta H(T)$	$-T\Delta S(T)$	$\Delta G_{th}(T)$[i]
EtOH									
trans[f]	0.00	0.00	0.00	0.00	0.00	0.00	0.00	0.00	0.00
gauche	0.03	−0.35	−0.32	0.05	−0.31	−0.26	0.77	−0.82	−0.05
i-PrOH									
trans[g]	0.00	0.00	0.00	0.00	0.00	0.00	0.00	0.00	0.00
gauche	0.00	−0.41	−0.41	0.01	−0.42	−0.41	−0.01	−0.39	−0.40
i-BuOH									
Tt[h]	0.00	0.00	0.00	0.00	0.00	0.00	0.00	0.00	0.00
Tg	0.07	−0.32	−0.25	0.10	−0.28	−0.18	0.16	−0.28	−0.14
Gt	−0.06	−0.49	−0.55	−0.06	−0.46	−0.52	−0.02	−0.43	−0.45

[a] Energies are given in kilocalories per mole. [b] Gas-phase B3LYP/6-31G* calculations with geometry optimization. [c] Gas-phase B3LYP/6-311++G**//B3LYP/6-31G* single-point calculations. [d] PCM/B3LYP/6-31G* in-solution calculations with geometry optimization. [e] PCM/B3LYP/6-311++G**//PCM/B3LYP/6-31G* single-point in-solution calculations. [f] CCOH gauche and trans structures. [g] HCOH gauche and trans structures. [h] For the T, G, t, and g letter codes for the *i*-BuOH conformers, see the text. [i] $\Delta G_{th}(T) = \Delta H(T) - T\Delta S(T)$ was calculated for the geometry-optimized structure at the B3LYP/6-31G* level in the gas phase and in the corresponding solvent.

the composition more closely to the experimental one than by the 6-311++G** basis set. This result confirmed our previous selection in favor of the 6-31G* basis set for charge derivation.

For in-solution equilibria, the relative energies in the upper part of Table 4 stand for the $\Delta E(\text{int}) + \Delta G(\text{solv})$ energy sum, whereas the remaining terms in eq 3b are collected in $\Delta G_{th}(T)$. Thus, $\Delta G_s^o = \Delta E(\text{int}) + \Delta G(\text{solv}) + \Delta G_{th}(T)$ when the energy contributions are taken from Table 4. Considering the EtOH conformational equilibrium in solution, both basis sets predict the prevalence of the gauche EtOH conformer in acetonitrile and in water. The calculated free energy differences are in the range of 0.30−0.66 and 0.46−0.53 kcal/mol in acetonitrile and water, respectively. These differences allow the presence of a considerable trans fraction but generally slightly smaller than predicted by the corresponding gas-phase calculations.

For *i*-PrOH, the two basis sets predict different signs for the relative energies in the gas phase and in acetonitrile but agree that the trans conformer is the lower internal energy [including $\Delta G(\text{solv})$] structure in water. The $\Delta G_{th}(T)$ term is uniformly about −0.41 kcal/mol, making the gauche structure more favorable in any environment.

Regarding the Gt conformation of *i*-BuOH, the calculation results are unequivocal. From internal energy and thermal corrections, this conformer is the most stable out of the three structures considered, both in the gas phase and in solution. The sign for the relative internal energy is consistently different for the Tt and Tg conformers when the two basis sets are used. The 6-31G* results favor the Tg form over the Tt structure, while the 6-311++G** basis set predicts the opposite preference. Nonetheless, all three conformers may appear in the equilibrium mixture in a nonnegligible fraction, such that separate MC simulations have been performed for each structure.

Multiple Solvents in Continuum Dielectric Calculations. If the bulk dielectric constant can adequately characterize the solvent effect in mixtures, then a continuum dielectric approach would be very useful in calculating the energy (free energy) changes along a chemical reaction path. However, as described in the Methods section, the Gaussian implementation of the PCM method (even the most recent G03 version[11b]) does not accept mixed solvents. The situation can be approached by introducing another parameter, such as "number of solvent components", which would allow at least two solvent components to be considered. When such an approach is taken, the problem then becomes: what combination rule or other method should be used to define the *single* parameter set that best represents the mixed solvent?

A more basic question is whether such an approach is physically sound. One can easily imagine that a solute would discriminate the mixed solvent molecules wherein some sites would favor one type of solvent while other sites would favor a different solvent component. Thus, a continuum dielectric solvent program might model the mixed solvent in a physically more realistic way by allowing a ranking of the solvent components at user-defined solute sites. In this case, every site would be solvated by the highest-rank solvent present in the mixture, according to user-defined or program-suggested priorities. The program would then stipulate the requested parameter combination at the respective sites.

In Chart 1, a flowchart is presented outlining our suggested approach. In step 1, the user defines two or more solvent components (by names) comprising the mixed solvent. In the example, the solvent consists of three components: benzene, methanol, and acetonitrile. No specification for the composition of the mixed solvent is required. The basic idea of the present suggestion is that the solvent components can have the option

CHART 1

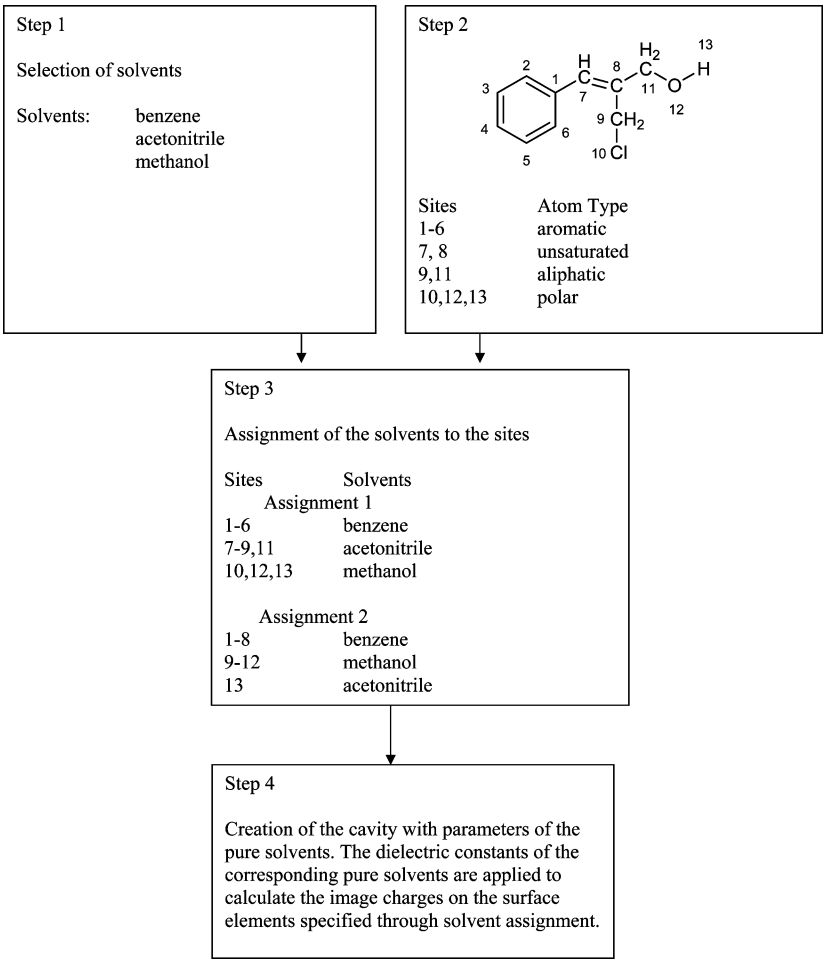

to solvate the solute in its first solvation shell with a local composition that may be different from the stoichiometric ratio for the bulk mixed solvent. In step 2, the solute's atom groups are assigned as polar, aliphatic, unsaturated, or aromatic sites. An example is given where the solute molecule includes all site types. Atoms in the CH_x groups are to be considered separately. Step 3 is the key feature of the present model, wherein the solvent components are selectively assigned to the prespecified atom sites on the solute. Thus, for example, the polar O, H, and Cl groups can be appropriately solvated by methanol, the aromatic CHs can be solvated by benzene, and the aliphatic and unsaturated sites can be solvated by acetonitrile (assignment 1). Although an expert system for such assignments would be ultimately very useful, its development will need many calculations and reiterations of this method. Even then, however, it would remain a useful option for assignments to still be able to be made by a user. By this option, the user can test ideas about the different chemical behavior that might result upon "unusual" solvent assignment. Consideration of the solute conformation is an important issue, as well. In case of the possibility of an internal hydrogen bond, the solvation pattern may be different for conformers with and without this bond.

Step 4 is the application of the present PCM procedure for the system developed in steps 1−3. The cavity will be created around all solute sites with the corresponding parameters of the assigned solvent. In the SCF process for finding the surface charges, the dielectric constant of the pure solvent specified in the site-solvation assignment step is to be used for the elements belonging to the solvation surface of the given site.

With any conformations or tautomeric forms for the solute and throughout any assignments of the solvent components to the atom sites on the solute, one may tacitly assume that the model refers to the same macroscopic system, thus comparison of the different micromodels are justified. In this case, however, the lowest free energy model calculated by the PCM method would indicate the most relevant solute structure and solvation pattern in the present approach. When a continuum dielectric model is applied, however, the free energy contribution due to the solvent reorganization upon the different solvent assignments cannot be taken into consideration.

Monte Carlo Simulations. To interpret the Monte Carlo results, structures and energies of alcohol−solvent dimers were optimized by using the 12-6-1 pair-potential as described in the Methods section (Table 5). The calculated H···O hydrogen-bond distances in the alcohol−water pairs (considering the TIP4P model) are about 1.80 Å, irrespective of whether the alcohol (H_a) or the water (H_w) provides the donor atom in the hydrogen bond. The O−H···O angles are in the 166−180° range; thus the bonds are slightly bent for the studied dimers even in their most favorable orientations.

With the three-point acetonitrile model, only the H_a···N hydrogen bond is possible. The distance is approximately 1.9 Å, or about 0.1 Å longer than in the alcohol−water dimers. The O−H···N angle is 166−180°. Thus, this H-bond is also only slightly bent. Acetonitrile is a linear molecule and in this case the H···N−C angle is also important. Table 5 shows that this molecular axis does not coincide with the (almost) linear O−H···N axis. Furthermore, the H···N−C angle changes

TABLE 5: Optimized Geometric Parameters and Interaction Energies for Dimers, Calculated by Using the 12-6-1 Interaction Potential[a]

	distances (Å)			angles (deg)			
	water (TIP4P) $H_a\cdots O_w$	water (TIP4P) $O_a\cdots H_w$	MeCN $H_a\cdots N$	water (TIP4P) $O_a-H_a\cdots O_w$	water (TIP4P) $O_a\cdots H_w-O_w$	MeCN $O_a-H_a\cdots N$	MeCN $H_a\cdots N-C$
EtOH							
gauche[b]	1.77	1.79	1.91	174	178	176	137
trans	1.77	1.77	1.91	179	180	179	148
i-BuOH							
Tt[c]	1.75	1.81	1.89	178	174	180	159
Tg	1.80	1.80	1.95	166	178	166	125
Gt	1.75	1.84	1.89	178	167	180	155
i-PrOH							
gauche[d]	1.77	1.79	1.92	177	180	174	128
trans	1.77	1.78	1.92	178	180	175	127
t-BuOH	1.78	1.79	1.92	178	177	175	126

	interaction energies (kcal/mol)								
	water (TIP4P) $H_a\cdots O_w$			water (TIP4P) $O_a\cdots H_w$			MeCN $H_a\cdots N$		
	E_{elst}	E_{vdw}	E_{tot}	E_{elst}	E_{vdw}	E_{tot}	E_{elst}	E_{vdw}	E_{tot}
EtOH									
gauche[b]	−8.17	1.40	−6.77	−8.04	1.59	−6.45	−5.22	−0.02	−5.24
trans	−8.03	1.51	−6.52	−8.35	1.64	−6.71	−5.15	0.24	−4.91
i-BuOH									
Tg[c]	−7.08	1.11	−5.99	−7.90	1.32	−6.58	−4.79	−0.40	−5.19
Tt	−8.56	1.65	−6.91	−7.39	1.12	−6.27	−5.52	0.28	−5.24
Gt	−8.55	1.66	−6.89	−7.38	1.11	−6.27	−5.49	0.29	−5.20
i-PrOH									
gauche[d]	−8.17	1.37	−6.81	−8.31	1.41	−6.90	−5.08	−0.20	−5.27
trans	−8.04	1.20	−6.84	−8.16	1.59	−6.57	−4.99	−0.40	−5.39
t-BuOH	−7.93	1.13	−6.80	−8.44	1.39	−7.05	−5.02	−0.49	−5.51

[a] E_{elst} and E_{vdw} energies correspond to the Coulomb and Lennard-Jones terms, respectively, in the 12−6−1 potential function. [b] CCOH gauche and trans structures. [c] For the T, G, t, and g letter codes for the *i*-BuOH conformers, see the text. [d] HCOH gauche and trans structures.

considerably for the different alcohols, namely, in the 125−159° range for primary alcohols compared to 126−128° for secondary and tertiary alcohols.

As far as the dimer energies are concerned, no clear trend has been found whether the $H_a\cdots O_w$ or the $H_w\cdots O_a$ hydrogen bond is the preferred type of monohydration. The total interaction energies, E_{tot}, are in the −6.0 to −7.1 kcal/mol range. The preference of the hydrogen bond switches with gauche and trans conformations for both EtOH and *i*-PrOH. Furthermore, different hydrogen bonds are favored for the gauche conformations as well as for the trans conformations when the corresponding hydrogen bonds are compared for EtOH and *i*-PrOH. Nonetheless, the differences in E_{tot} are small, amounting to only a few tenths of a kilocalorie per mole. Likewise, no single hydrogen-bond type is favored for the three *i*-BuOH conformers, but the differences in the two hydrogen-bond E_{tot} values at a specific solute conformation amount to about 0.6 kcal/mol. The E_{tot} values differ by 0.25 kcal/mol in the *t*-BuOH−water dimers. Common in all alcohol−water interactions is that the electrostatic term is the dominant one, whereas the E_{vdw} term accounting for the nonelectrostatic interactions is always of positive sign.

The alcohol−MeCN interaction energies range between −4.9 and −5.5 kcal/mol and are weaker than the alcohol−water interactions by 0.8−1.7 kcal/mol for a given solute conformer. The electrostatic component is again the dominant term in the case of the dimers with MeCN. With this solvent molecule, however, the E_{vdw} term can also be negative, as was found mainly for the secondary and tertiary alcohols.

When the solution models with 263−508 solvent molecules in Monte Carlo simulations are considered (Table 6), the average E_{elst} interaction energies are −19.5 to −23.7 kcal/mol for the alcohols in pure water. The electrostatic terms for the gauche conformers are slightly more negative than those for the corresponding trans conformations. E_{elst} for primary alcohols is generally less negative than that for the secondary and tertiary alcohols. The CCCO conformation is important for *i*-BuOH: in its Gt form the E_{elst} value is almost the most negative one in the studied series.

E_{elst} for alcohols is uniformly about −6 kcal/mol in acetonitrile. This can be interpreted by assuming a single $O-H\cdots N$ hydrogen bond between any alcohols in the solution and a close acetonitrile solvent molecule. The −6 kcal/mol value is slightly more negative than the E_{elst} term for the optimized dimers. It suggests that more than one close acetonitrile molecule contributes favorably to the electrostatic interactions.

Whereas the electrostatic term is always the dominant contribution to the total interaction energy for different *dimers*, the van der Waals term may become the prevailing component of the average total solute−solvent interaction energy calculated as the sum of interaction energies between the single solute and each solvent molecule within spheres (R = SCUT = 12 Å) around any solute atoms. The 12 Å solute−solvent cutoff radius ensures consideration of more than 50% of the solvent molecules in the solvent box. The E_{vdw} terms are remarkable even in water and become gradually more negative with an increasing number of atoms in EtOH, *i*-PrOH, and butyl alcohols. For *i*-BuOH and *t*-BuOH, the E_{vdw} value is very close, indicating that the dispersion interaction depends primarily on the number of atoms in the solute and changes little with the chemical constitution. E_{vdw} was calculated from the $A/r^{12} - B/r^6$ Lennard-Jones term of the OPLS interaction potential. Constants A and B are posi-

TABLE 6: Solute−Solvent Interaction Energies in Pure Solvents and Water−Acetonitrile Mixtures[a]

	EtOH	*i*-BuOH	*i*-PrOH	*t*-BuOH	isopentene
			Water, $N = 508$		
	gauche[b]	Tg[c]	gauche[d]		
E_{elst}	−22.1 ± 0.3	−21.2 ± 0.3	−23.7 ± 0.4	−23.3 ± 0.5	−4.1 ± 0.2
E_{vdw}	−2.9 ± 0.1	−6.7 ± 0.1	−5.2 ± 0.1	−6.5 ± 0.1	−9.9 ± 0.1
E_{tot}	−25.0 ± 0.3	−27.9 ± 0.2	−28.9 ± 0.3	−29.8 ± 0.4	−14.0 ± 0.2
	trans[b]	Tt[c]	Gt[c]	trans[d]	
E_{elst}	−20.6 ± 0.3	−19.5 ± 0.3	−23.6 ± 0.3	−23.4 ± 0.4	
E_{vdw}	−2.9 ± 0.1	−6.8 ± 0.1	−6.7 ± 0.1	−5.1 ± 0.1	
E_{tot}	−23.5 ± 0.2	−26.3 ± 0.2	−30.3 ± 0.2	−28.5 ± 0.3	
			Water/Acetonitrile = 70:30, $N = 356 + 152$		
	gauche	Tg	Gt		
E_{elst}	−15.7 ± 0.4	−11.3 ± 0.2	−15.7 ± 0.3		−1.4 ± 0.1
E_{vdw}	−5.2 ± 0.1	−11.0 ± 0.1	−8.9 ± 0.1		−12.3 ± 0.1
E_{tot}	−20.8 ± 0.3	−22.3 ± 0.2	−24.6 ± 0.2		−13.6 ± 0.1
			Water/Acetonitrile = 50:50, $N = 254 + 254$		
	gauche	Tg	gauche		
E_{elst}	−14.2 ± 0.3	−15.2 ± 0.2	−14.2 ± 0.2	−15.2 ± 0.3	−0.6 ± 0.1
E_{vdw}	−5.6 ± 0.1	−10.0 ± 0.1	−8.5 ± 0.1	−10.1 ± 0.1	−13.8 ± 0.1
E_{tot}	−19.8 ± 0.2	−25.2 ± 0.2	−22.7 ± 0.3	−25.3 ± 0.2	−14.3 ± 0.1
	trans	Tt	Gt	trans	
E_{elst}	−14.8 ± 0.3	−16.3 ± 0.2	−10.4 ± 0.4	−16.0 ± 0.3	
E_{vdw}	−5.3 ± 0.1	−10.2 ± 0.1	−11.4 ± 0.1	−7.8 ± 0.1	
E_{tot}	−20.1 ± 0.2	−26.5 ± 0.2	−21.8 ± 0.3	−23.8 ± 0.3	
			Water/Acetonitrile = 30:70, $N = 79 + 184$		
	gauche	Tg	gauche		
E_{elst}	−11.0 ± 0.3	−12.5 ± 0.3	−10.9 ± 0.2	−15.3 ± 0.3	−1.6 ± 0.1
E_{vdw}	−7.2 ± 0.1	−11.1 ± 0.1	−9.9 ± 0.1	−10.6 ± 0.1	−14.2 ± 0.1
E_{tot}	−18.2 ± 0.3	−23.5 ± 0.2	−20.7 ± 0.2	−25.9 ± 0.2	−15.8 ± 0.1
	trans	Tt	Gt	trans	
E_{elst}	−8.9 ± 0.3	−6.9 ± 0.1	−10.7 ± 0.3	−8.2 ± 0.2	
E_{vdw}	−7.8 ± 0.1	−13.1 ± 0.1	−12.3 ± 0.1	−10.9 ± 0.1	
E_{tot}	−16.7 ± 0.3	−20.0 ± 0.1	−22.9 ± 0.2	−19.2 ± 0.2	
			Water/Acetonitrile = 20:80, $N = 53 + 210$		
	gauche				
E_{elst}	−14.0 ± 0.2				
E_{vdw}	−6.2 ± 0.1				
E_{tot}	−20.2 ± 0.1				
			Water/Acetonitrile = 10:90, $N = 26 + 237$		
	gauche	Tt	Gt	trans	
E_{elst}	−11.6 ± 0.3	−6.4 ± 0.1	−7.6 ± 0.2	−9.0 ± 0.1	−6.9 ± 0.2 (−6.7 ± 0.2)[e]
E_{vdw}	−6.8 ± 0.1	−13.0 ± 0.1	−12.9 ± 0.1	−9.9 ± 0.1	−12.9 ± 0.1 (−13.0 ± 0.1)[e]
E_{tot}	−18.4 ± 0.2	−19.4 ± 0.1	−20.5 ± 0.2	−18.9 ± 0.1	−19.8 ± 0.2 (−19.7 ± 0.1)[e]
			Acetonitrile, $N = 263$		
	gauche	Tg	gauche		
E_{elst}	−6.1 ± 0.1	−5.9 ± 0.1	−6.0 ± 0.1	−6.2 ± 0.1	−0.7 ± 0.1
E_{vdw}	−8.4 ± 0.1	−13.4 ± 0.1	−11.0 ± 0.1	−13.0 ± 0.1	−13.6 ± 0.1
E_{tot}	−14.5 ± 0.1	−19.3 ± 0.1	−17.0 ± 0.1	−19.2 ± 0.1	−14.3 ± 0.1
	trans	Tt	Gt	trans	
E_{elst}	−6.0 ± 0.1	−6.0 ± 0.1	−6.4 ± 0.1	−6.3 ± 0.1	
E_{vdw}	−8.5 ± 0.1	−13.1 ± 0.1	−13.6 ± 0.1	−11.3 ± 0.1	
E_{tot}	−14.5 ± 0.1	−19.1 ± 0.1	−20.0 ± 0.1	−17.6 ± 0.1	

[a] Energies are given in kilocalories per mole. $E_{tot} = E_{elst} + E_{vdw}$. Values are derived from averaging 7.5 M configurations. [b] CCOH gauche and trans structures. [c] For T, G, t, and g letter codes, see the text. [d] HCOH gauche and trans structures. [e] Averages in parentheses were calculated by considering 12.5 M configurations.

tive values for any atom pairs such that negative E_{vdw} values indicate that the $-B/r^6$ dispersion term dominates the so-called van der Waals interactions between the solute and the solvent molecules.

In acetonitrile solvent, the E_{vdw} interactions provide the dominant contribution to the total interaction energy. Again, the E_{vdw} values become more negative for solutes with increasing number of atoms in the molecule. E_{vdw} does not show a remarkable dependence on conformations in either pure water or acetonitrile.

The above findings suggest that there may be gradual changes for the energy components in mixed solvents, although this has not been calculated in every case. E_{elst} is greatly reduced (less negative) for alcohols when the solvent contains at least 50% acetonitrile compared to pure water. The E_{vdw} terms become more negative and further show the aforementioned dependence on the number of atoms within the solute. Whereas dramatic changes (decrease in absolute value) have been calculated in the E_{elst} terms for the *i*-BuOH Tt and the trans *i*-PrOH conformers when the composition is changed from water:acetonitrile = 50:50 (henceforth w:acn = 50:50) to w:acn = 30:70, the average electrostatic interaction energy remains unchanged for *i*-BuOH Gt and *t*-BuOH in these mixtures. A detailed study for the gauche EtOH conformer in w:acn = 20:

80 and 10:90 mixtures shows that the avarge E_{elst} value does not change monotonically: E_{elst} is −14 kcal/mol in w:acn = 20:80 and is about −11 kcal/mol in both w:acn = 30:70 and 10:90 mixtures. E_{elst} also does not change monotonically for the *i*-BuOH Tg conformer in the water 100%−50% range. All these results indicate that the actual solvation pattern is a delicate interplay of the solute conformation and the solvent composition.

The calculated standard deviations for E_{elst} are only a few percent of the mean data for the water-containing mixtures, thus a stable average must have been calculated. The nonmonotonic change of the average values can be interpreted by assuming that either the different systems remained trapped in different local minima or the nonmonotonic change of E_{elst} is an inherent feature of the studied systems. This question is more closely addressed in the next section.

Table 6 summarizes the energy results for the 3-methylbut-1-ene (isopentene) solute as well. This molecule has the same number of heavy atoms as the butyl alcohols and is structurally close to *i*-BuOH: the $-CH_2-OH$ moiety changes to $-CH=CH_2$. This hydrocarbon does not have an obvious site for the formation of a classical hydrogen bond when the weak $C-H\cdot\cdot\cdot O_w$ bonds[21] are disregarded. A weak interaction of the π electrons of the C=C double bond and the water hydrogen is possible, however, similar to that found for the benzene−water dimer.[22] In fact, Tarakeshwar et al.[23] pointed out that the binding energy of the ethene−water dimer is smaller than that of the benzene−water dimer only by about 1 kcal/mol. In our approach, the double bond was not explicitly considered, but the derived atomic charges for the $-CH=CH_2$ moiety account for the electron distribution of a C=C double bound. The MC simulations predict weak solute−solvent electrostatic interactions as was concluded from the strong decrease (in absolute value) of the E_{elst} terms in Table 6. In contrast, E_{vdw} is close to the corresponding value for butyl alcohol isomers, especially in solvents with large fractions of acetonitrile. These results suggest that the present model is responsive to a decrease of the electrostatic stabilization when the solute forms only a weak hydrogen bond. On the other hand, the van der Waals interaction energy is at least as negative as in the cases of the alcoholic solutes having equal numbers of heavy atoms and hydrogens.

Structure of the First Solvation Shell. In this paper we have examined whether such "solvent discrimination" does indeed exist by deploying short-chain alcohols in water−acetonitrile mixtures as simple test systems. The starting points of our study are solutions in pure solvents wherein there is no solvent competition and the solvent molecules should surround the solute in some energetically favorable way. The BOSS program uses the Metropolis test[15b] for accepting or rejecting a new configuration. This procedure ensures that the energies of the configurations show the Boltzmann distribution. The statistical parameters for the equilibrated system are stable when the thermodynamic variables are calculated. While a necessary condition for equilibrium, it should be noted that the obtainment of stable average values for the calculated thermodynamic parameters (even when large fluctuation is allowed for) does not rule out that the system remains trapped in some arrangements of local energy minimum character. Only long simulations with several returns of structural arrangements suggest truly equilibrated systems.

From Table 5, the electrostatic interaction energy is about −8 kcal/mol for dimers with water. The largest one-solvent contribution to the total solute−solvent electrostatic energy comes from the nearest solvent molecules, that is, from those in the first solvation shell. In this region, alcohols tend to have

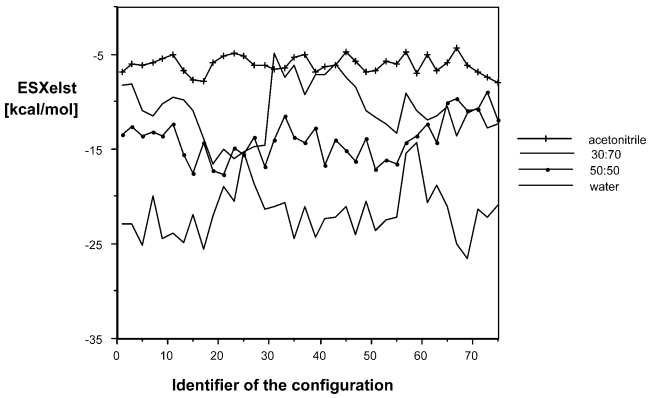

Figure 1. Change of the solute−solvent electrostatic interaction energy (ESXelst) in the averaging phase for the gauche EtOH in pure solvents and in w:acn = 50:50 and 30:70 mixtures. Standard deviations for the average values are 0.3 and 0.1 kcal/mol in water-containing solvents and pure acetonitrile, respectively (Table 6).

two or three water molecules around the OH group in pure water, most of them being hydrogen-bonded to the solute (see below). On the basis of the calculated value for the dimer, removal of a water molecule from the first hydration shell will considerably decrease the electrostatic stabilization, and the effect should be reflected in a less negative average E_{elst} value even if an acetonitrile replaces the water molecule in the $O_a-H_a\cdots O_w$ bond by forming a new $O_a-H_a\cdots N$ bond.

The subaverage E_{elst} values from 75 consecutive steps are shown in Figure 1 for the gauche EtOH conformer in four different solvents. The E_{elst} values show fluctuations of several kilocalories per mole around the final average of -22.1 ± 0.3 kcal/mol in pure water (Table 6). The fluctuation is much smaller in pure acetonitrile around the final average value of -6.1 ± 0.1 kcal/mol. Medium fluctuations were found in the w:acn = 50:50 solvent, but large and *long-lasting* deviations were found in w:acn = 30:70. The final E_{elst} value in this solvent is -11.0 ± 0.3 kcal/mol. The subaverages are about −15 kcal/mol in the step range of 20−30 and jump to about −7 kcal/mol at step 31. This value, with the exception of a short decrease around step 37, is maintained in the step range of 33−43. After that, the subaverages fluctuate around the final average until the end of the simulation at step 75.

If a large energy decrease is calculated for a system and the system does not, with time, return to the former state, one may expect that a high-energy state (perhaps a high-lying local energy minimum) was vacated. A return suggests, however, that the state in question is reachable from lower energy states. The E_{elst} subaverage values are around −10 kcal/mol at the onset of the averaging phase in the w:acn = 30:70 solvent. A decrease and a sudden increase followed eventually by fluctuation of E_{elst} around the final average indicates that large energy changes are still possible for this solution even after a long equilibration phase. The return to the average, however, suggests that the system has basically equilibrated.

One must then ask what causes the jump of about 8 kcal/mol at step 31. A possible interpretation, based upon the calculations of the dimers, is that a water molecule left the shell around the alcoholic OH. Implicit in this explanation is that there *had been* a water molecule in the solvation shell of the alcoholic group, even in a solvent containing 70% (molar fraction) acetonitrile and only 30% water.

Interpretation of Figure 2 leads to the conclusion that there can be at least one water molecule around *t*-BuOH even in a solvent w:acn = 10:90. E_{elst} subaverages for *t*-BuOH show large, small, and medium fluctuations around the corresponding final

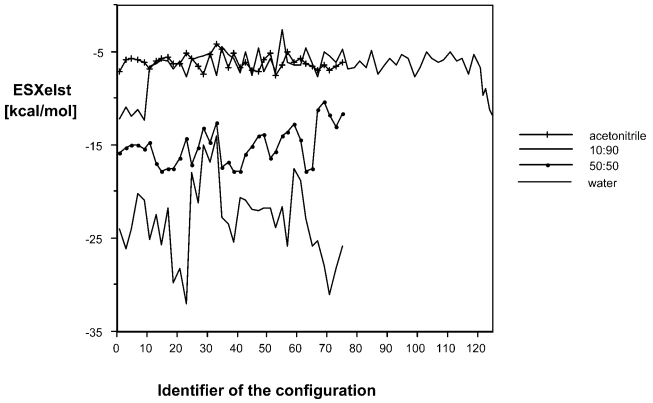

Figure 2. Change of the solute−solvent electrostatic interaction energy (ESXelst) in the averaging phase for *t*-BuOH in pure solvents and in w:acn = 50:50 and 10:90 mixtures. Standard deviations for the average values are 0.5, 0.3, 0.2, and 0.1 kcal/mol with decreasing water contents, respectively (Table 6).

averages in pure water, acetonitrile, and w:acn = 50:50, respectively. The E_{elst} trajectory for w:acn = 10:90 starts at about −12 kcal/mol, which is much below the −7 kcal/mol value calculated for most of the steps in the averaging phase. If E_{elst} decreases considerably, one may expect that the system has not reached equilibrium. But then why does the E_{elst} subaverage increase after such a long simulation? It was hypothesized that the system was in equilibrium but reached a higher energy state. In fact, an increase of about 5 kcal/mol in consecutive subaverages is not unusual. Much larger increases are accepted by the Metropolis test in the BOSS program, however, for subaverages of the total energy of the system. An increase of E_{elst} by about 5 kcal/mol again suggests that a water molecule left the alcoholic O−H area and the $OH_a\cdots O_w$ hydrogen bond was replaced by a $OH_a\cdots N$ bond with an acetonitrile solvent. Inspection of the graphical output confirmed this hypothesis. Thus, even at the onset of the averaging phase, there was a water molecule hydrogen-bonded to the *t*-BuOH solute in a solvent mixture having only 10% water. To prove that this solution structure is energetically affordable, an additional 50 steps were considered after the regular 75 steps in the averaging phase. The subaverage E_{elst} value returned to −11 kcal/mol at about step 123, and the graphical display indicated that E_{elst} decreased again precisely when a water molecule returned to the first solvation shell and formed a hydrogen bond to the *t*-BuOH alcoholic group. The combination of these results proves that a water molecule in the first solvation shell of an alcohol is energetically affordable even when the water molar fraction is low in the system. The most important conclusion from the above two examples regarding the gauche EtOH conformer and *t*-BuOH in low water-fraction mixed solvents is that the solute environment will not be represented well in continuum solvent quantum chemical methods if the bulk dielectric constants near that for pure acetonitrile are applied for these mixtures.

Figure 3 emphasizes the importance of the solute conformation in mixtures. In the w:acn = 50:50 solvent, the solute−solvent electrostatic interaction can be fairly different for the *i*-BuOH conformers. The E_{elst} subaverages moderately oscillate about the final averages of −16 and −15 kcal/mol for the CCCO trans Tt and Tg conformers, respectively. The CCCO gauche Gt structure has about − 6 kcal/mol solute−solvent electrostatic interaction energy in the configuration range of 40−60. These relatively high energy E_{elst} subaverages may be interpreted by an enhanced fraction of the H···N instead of the H···O hydrogen bonds for this conformer. No such high E_{elst} region has been

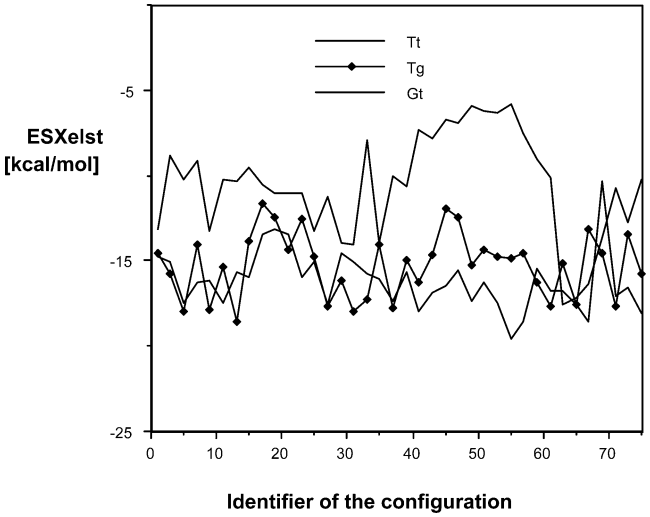

Figure 3. Change of the solute−solvent electrostatic interaction energy (ESXelst) in the averaging phase for the *i*-BuOH conformers in w:acn = 50:50 mixtures. Standard deviations for the average values are 0.2, 0.2, and 0.4 kcal/mol with the Tg, Tt, and Gt solutes, respectively (Table 6).

calculated for the Tt and Tg conformers, suggesting different solvation of these conformers in a w:acn = 50:50 solvent.

By molecular dynamics simulations, Kovacs and Laaksonen[24] studied the structure of the binary water−acetonitrile mixtures at different compositions. These authors found that the "acetonitrile structure remains relatively intact in the aqueous solutions. At low acetonitrile content, the close arrangement of the acetonitrile molecules with their dipoles antiparallel, remains." At the other end, when the water concentration is small in acetonitrile (water molar fraction is 0.12), the radial correlation of water enhances. This finding was rationalized by the presence of water dimers (H−O−H···H−O−H), trimers, etc., rather than by an extensive hydrogen-bonded network prevalent in pure water. Our simulation results with water molar fractions of 0.3−0.1 show a gradual shift of the solution structures from a hydrogen-bonded network pattern to a structure with water clusters of 2−6 water molecules.

Aqueous solution of *t*-BuOH has been simulated by means of both the Monte Carlo and molecular dynamics methods. In MC simulations of Nakanishi et al.,[25] a single *t*-BuOH solute was considered in a box of 215 water molecules. Those results are in accord with the predicted structure for the first hydration shell from the present study (see next section). When seven *t*-BuOH molecules were considered in a box of 209 water molecules in an MD simulation,[26] a clear association of the alcohol molecules was observed, without, however, formation of intermolecular hydrogen bonds between the solute molecules. More recent MD simulations for the characterization of the structure of dilute aqueous solutions of *t*-BuOH show that the obtained results are sensitive to the molecular model and the interaction potential adopted.[27] The finding that there is a cluster formation of *t*-BuOH in aqueous solution at about 0.03 molar fraction[26] does not invalidate the present results obtained with a single solute. Discrimination of the solvent's components by the solute can exist as long as there is no intermolecular hydrogen-bond formation between the alcohol molecules in the solution.

The $g(R)$ radial distribution functions (rdfs)[28] were calculated for the gauche EtOH conformer and *t*-BuOH in pure solvents. Figures 4−6 are qualitatively similar for the small primary and tertiary alcohols. The first peaks and minima of the $(O_a)H_a\cdots$

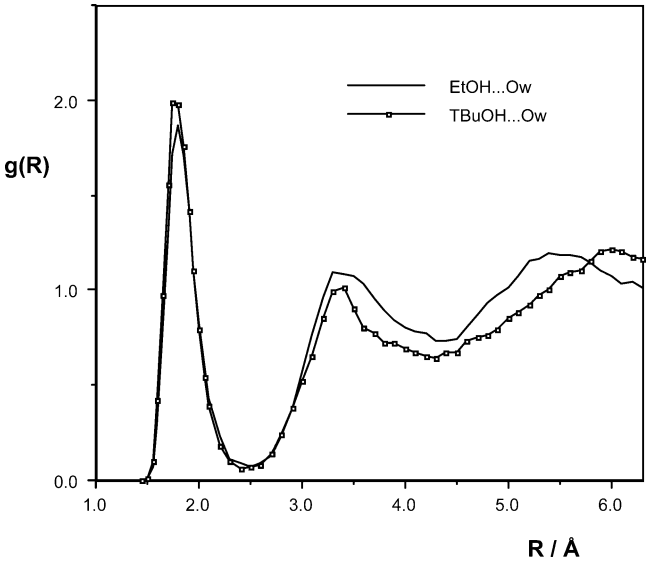

Figure 4. (O)H···O_w radial distribution functions for the gauche EtOH and *t*-BuOH in pure water.

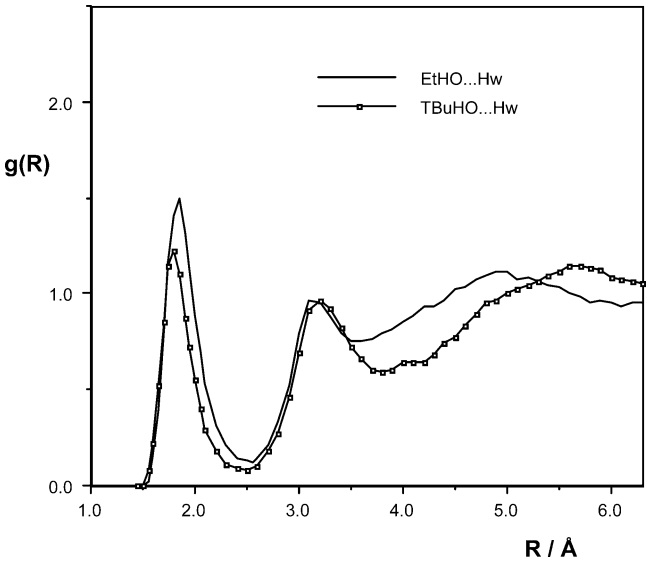

Figure 5. (H)O···H_w radial distribution functions for the gauche EtOH and *t*-BuOH in pure water.

O_w rdfs (Figure 4) are at $R = 1.75-1.80$ and $2.40-2.50$ Å, respectively, for the two alcohols. Integration of the $4R^2\pi g(R)$ function until the first minimum of $g(R)$ provides one hydrogen-bond acceptor water molecule for each alcohol in the first hydration shell. The well-resolved second peak of the $H_a\cdots O_w$ rdf stems from the oxygens of the donor water molecules forming the $O_a\cdots H_w-O_w$-type hydrogen bond to the alcoholic oxygen. The $H_a\cdots O_w$ distance for this optimized dimer in Table 5 is 3.32 Å, allowing interpretation of the second peak at about $R = 3.3$ Å.

The $(H_a)O_a\cdots H_w$ rdfs (Figure 5) have their first maxima and minima at $R = 1.80-1.85$ and $2.50-2.55$ Å, respectively. The first peaks in these rdfs are, however, not as high as in Figure 4, suggesting less stably localized water molecules forming the $O_a\cdots H_w-O_w$ hydrogen bonds. This finding is in accord with the less negative calculated interaction energy when the corresponding dimers for the gauche EtOHconformer are compared, but this simple explanation does not hold for *t*-BuOH. Integrations of the $4R^2\pi g(R)$ functions until the first minima predict 1.9 and 1.3 water molecules forming $O_a\cdots H_w-O_w$ hydrogen bonds to ethanol and *tert*-butyl alcohol, respectively. Thus,

TABLE 7: Number of Hydrogen Bonds to the Solute Calculated by the Integration of the Pair-Energy Distribution Functions

		water/acetonitrile			
	water	70:30	50:50	30:70	acetonitrile
EtOH					
gauche[a]	2.7	2.1	1.7	1.5	0.8
trans	2.7		1.9	1.3	0.9
i-BuOH					
Tg[b]	2.6	1.9	2.0	1.7	0.8
Tt	2.1		1.9	0.8	0.8
Gt	2.4	1.8	1.4	1.1	0.8
i-PrOH					
gauche[c]	2.4		2.2	1.1	0.8
trans	2.3		2.1	0.9	0.8
t-BuOH	2.1		1.9	1.9	0.9

[a] CCOH gauche and trans structures. [b] For T, G, t, and g letter codes, see the text. [c] HCOH gauche and trans structures.

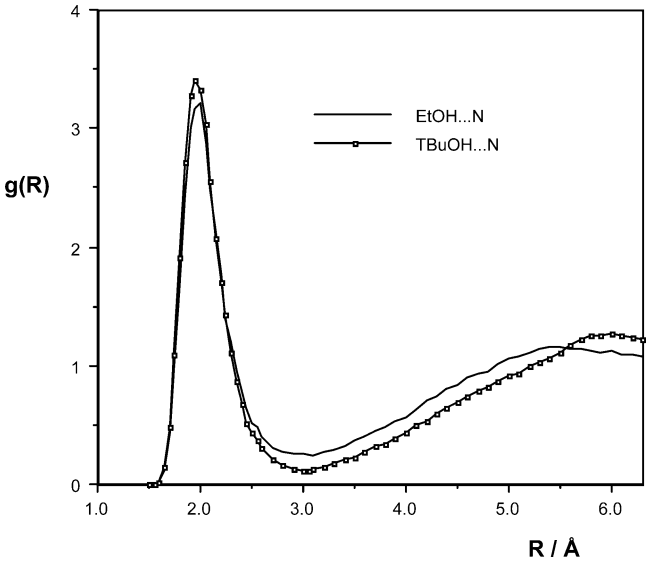

Figure 6. (O)H···N radial distribution functions for the gauche EtOH and *t*-BuOH in pure acetonitrile.

whereas the alcoholic group as a proton donor interacts with one water molecule in the case of either solute, ethyl alcohol accepts about 0.6 more hydrogen bonds, on average, than *tert*-butyl alcohol (Table 7). The smaller peak value for the (H_a)-$O_a\cdots H_w$ rdf compared to the $(O_a)H_a\cdots O_w$ rdf height for *t*-BuOH may be explained by assuming that although more than one water molecule is present in the first hydration shell, they mutually prevent each other from interacting with the solute as favorably as a single solvent can do it in the optimized dimer.

The two O−H···N rdfs run very close to each other in Figure 6. The peak values are above 3, as compared to 1.5−2.0 in Figures 4 and 5. The larger $g(R)$ peak value for H···N than for the alcohol−water interactions does not mean, however, that formation of an O−H···N hydrogen bond is energetically favored over an O−H···O_w bond. The $g(R)$ functions characterize the relative probability of the appearance of the H-bond acceptor atom at the alcoholic O−H site as compared to the bulk solvent. Thus, the $g(R)$ peak value may be larger for the acetonitrile N atom than for the water oxygen, due to a considerably enhanced local concentration of the nitrogen atom in the region, allowing formation of a hydrogen bond to an alcohol, compared to the bulk acetonitrile concentration.

The solute−solvent pair-energy distribution function (pedf)[14a,16] dN/dE as a function of E gives the number of solvent molecules

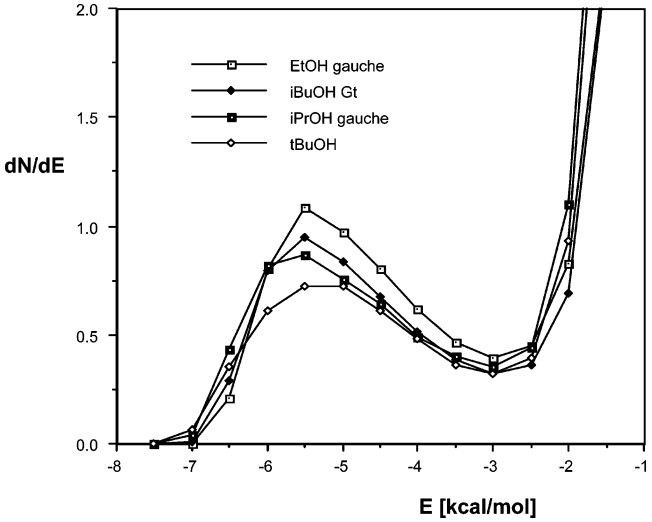

Figure 7. Pair-energy distribution functions for alcohols in pure water.

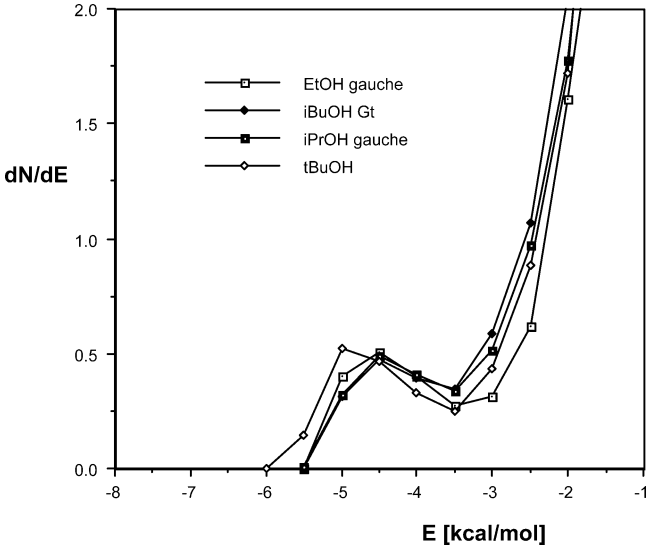

Figure 8. Pair-energy distribution functions for alcohols in pure acetonitrile.

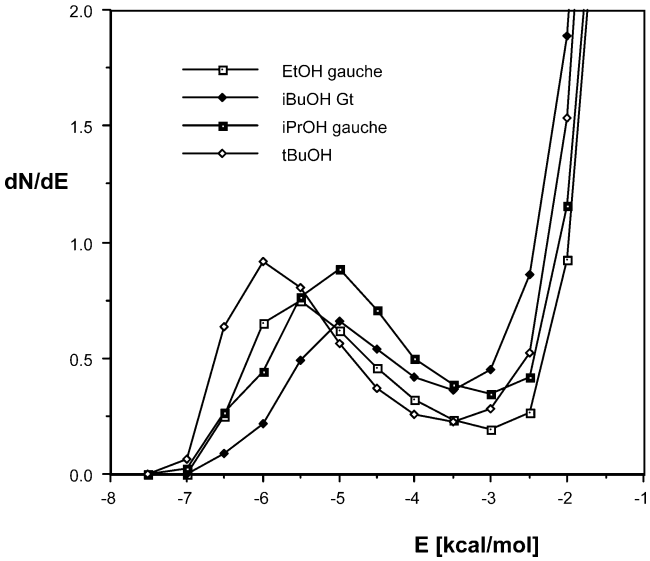

Figure 9. Pair-energy distribution functions for alcohols in the water: acetonitrile = 50:50 mixture.

(N) in energy interaction of $E \pm \Delta E$ with the solute. E corresponding to the lowest (nonzero) dN/dE value gives the most negative interaction energy between the solute and a *single* solvent molecule in solution. This value cannot be more negative than the optimized dimer interaction energy in Table 5. Instead, the onset value is most likely above this threshold because of thermal disordering.

Pedfs are provided for four alcohols as a function of the solvent composition in Figures 7−10. Data refer to the conformer of each solute that was found the be the most stable in pure solvents from conformational analysis (see the section above). The most negative pair interaction was calculated for *tert*-butyl alcohol in water (Figure 7). The onset E value is -7.00 ± 0.25 kcal/mol. The sampling energy range, ΔE, was set to 0.5 kcal/mol, and the data refer to the middle value in the range. The dN/d$E = 0$ value at $E = -7.5$ kcal/mol indicates that no pair-interaction energy was found in the range -7.50 ± 0.25 kcal/mol. Thus, the most negative calculated pair-interaction energy value is in the range of −7.25 to −6.75 kcal/mol. This range includes the energy value of −7.05 kcal/mol, the calculated optimized interaction energy for the *t*-Bu(HO)−HOH dimer. The simulation results indicate that only a very small fraction of the solvent molecules (dN/d$E = 0.06$ molecule/[kcal/mol], thus (dN/dE)$\Delta E = 0.03$ molecule out of the total 508 solvent water molecules) was found in the above range, which means that these solvent molecules are in nearly optimal arrangement for forming a hydrogen bond with the *tert*-butyl alcohol solute. For the other alcohols, dN/dE is practically zero at $E = -7$ kcal/mol, indicating that significant thermal disorder is in effect for these systems. The dimer energies would allow appearance of a water solvent in the −7.25 to −6.75 kcal/mol range for all three of the remaining alcohols.

The pedfs in Figure 7 show similar shapes, namely, that there is a maximum around $E = -5.5$ and a minimum at $E = -3$ kcal/mol. Former studies[5b,7,14a] indicated that the total number of alcohol−water hydrogen bonds can be estimated by integrating the dN/dE curve from the onset value until the first minimum. These integrals provide N_{HB} (number of hydrogen bonds) values of 2.7, 2.1−2.6, 2.3−2.4, and 2.1 for EtOH, *i*-BuOH, *i*-PrOH, and *t*-BuOH, respectively, in pure water (Table 7). It is interesting to note that EtOH can form a larger number of hydrogen bonds than the other primary alcohol, *i*-BuOH. Also interesting is that the tertiary and primary butyl alcohol in its Tt conformation form the same number of hydrogen bonds despite their different steric shielding of the OH group. Other *i*-BuOH conformers, Tg and Gt, however, form a remarkably larger number of hydrogen bonds. The N_{HB} values are, however, numbers obtained from the integration over the range. It is only the pedfs themselves that provide the precise energy distribution of the hydrogen bonds.

The pair-energy distribution energy for the four alcohols in pure acetonitrile is fairly uniform (Figure 8). The onset values are in the −5.75 to −5.25 kcal/mol range, in accord with the optimized alcohol−acetonitrile dimer interaction energies in Table 5. Integration of the curves until the minima at $E = -3.5$ kcal/mol provides about 0.8 acetonitrile molecule in hydrogen-bond to the alcoholic solutes (Table 7). This number is below the theoretically possible value of 1, indicating the moderate stability of the O−H···N hydrogen bond in solution.

In the w:acn = 50:50 solution (Figure 9), *t*-BuOH forms the strongest solute−solvent pair-interaction energy of the four structures considered. The peak for *t*-BuOH pedf is at $E = -6.0$ kcal/mol, and the pedf runs above all other until $E = -5.5$ kcal/mol. Beyond this point the gauche *i*-PrOH solute forms the most strong interactions. These results together explain that the N_{HB} values of 2.2 and 1.9 for gauche *i*-PrOH conformer and *t*-BuOH,

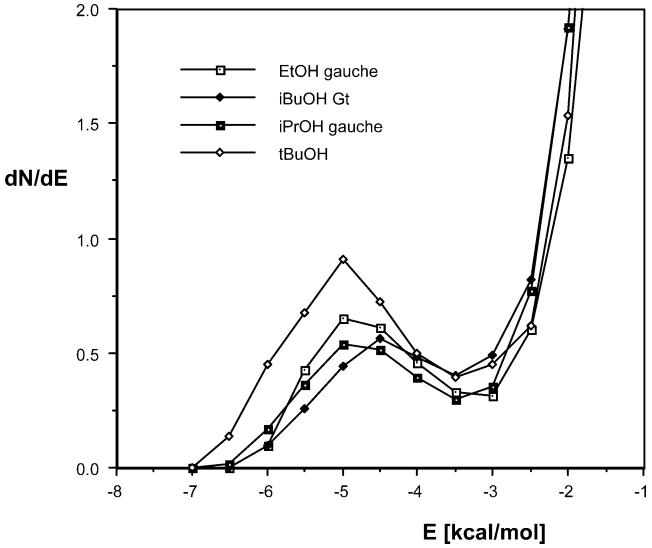

Figure 10. Pair-energy distribution functions for alcohols in the water: acetonitrile = 30:70 mixture.

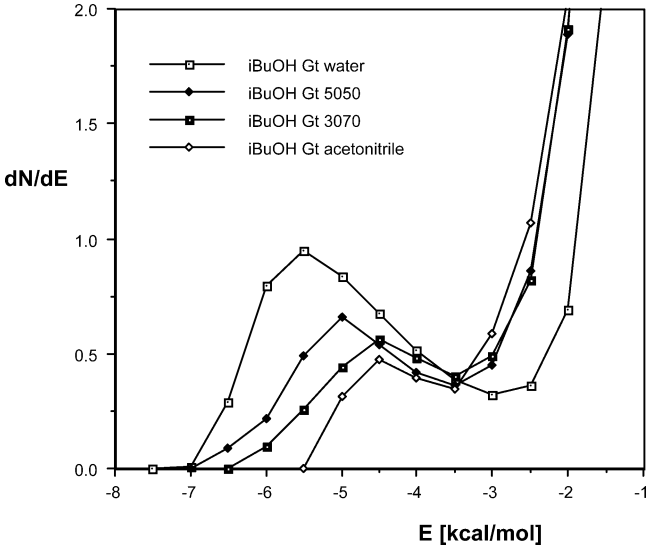

Figure 12. Pair-energy distribution functions for the *i*-BuOH Gt conformer in pure solvents and mixtures.

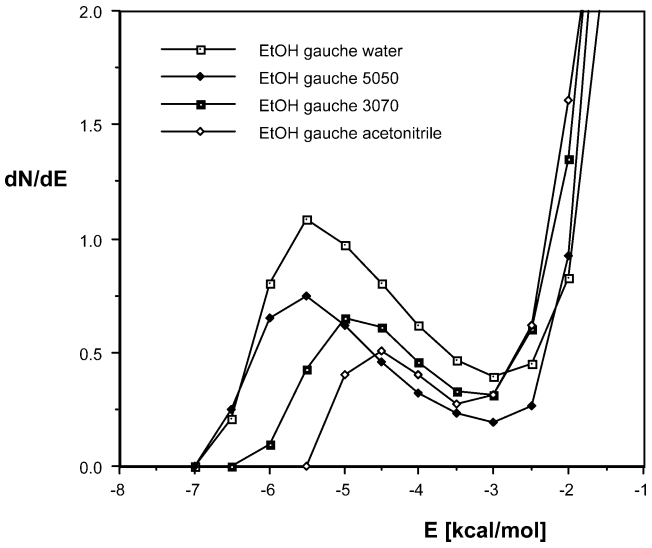

Figure 11. Pair-energy distribution functions for the gauche EtOH in pure solvents and mixtures.

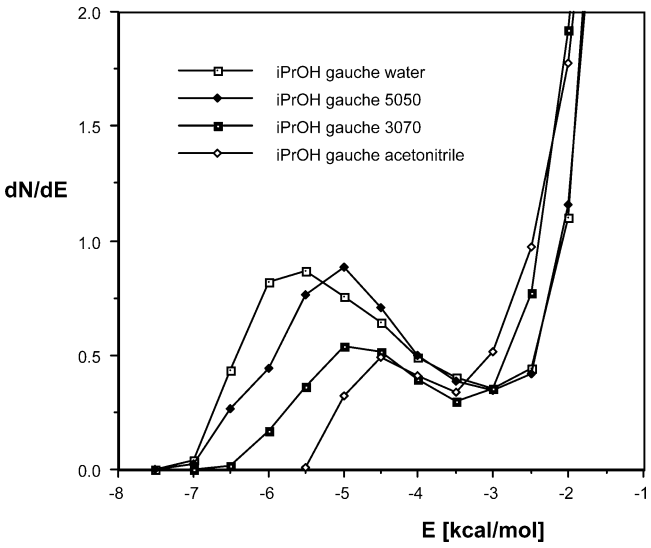

Figure 13. Pair-energy distribution functions for the gauche *i*-PrOH in pure solvents and mixtures.

respectively, are higher than those of 1.4−1.7 for the primary alcohols. The pedf is not indicated for the Tg and Tt *i*-BuOH conformers in Figure 9, for which solutes $N_{HB} = 1.9-2.0$.

Further increase of the acetonitrile fraction to w:acn = 30:70 leads to general right-hand shifts of the pedfs along the *E* axis (Figure 10). *t*-BuOH still forms the most negative interactions and presents the largest peak value of about 0.9 at $E = -5$ kcal/mol. The peaks are also located at this energy for EtOH gauche conformer and *i*-PrOH. The peak for the *i*-BuOH Gt conformer is identical to that in acetonitrile. The N_{HB} values scatter in the range of 0.9−1.9, indicating very different solvation in the first shell for the different solutes.

Figures 11−14 provide the pair-energy distribution functions for a specific alcohol in different solvents. Although all these figures can be constructed from curves presented in Figures 7−10, examination of Figures 11−14 is useful. Increase of the acetonitrile fraction results in a right shift of pedfs for all alcohols but *t*-BuOH (Figure 14). This finding calls attention to special circumstances during solvation of this alcohol in water−acetonitrile mictures. For the other alcohols/conformers, the onset values become gradually less negative and the peak values generally decrease and shift to the right.

All conclusions from Figures 7−14 suggest that equilibrium hydrogen-bond formation is a complicated problem in mixed water−acetonitrile solutions. The number of hydrogen bonds and the solute−solvent interaction energies are not always monotonic functions of the composition for the alcohols deployed in these studies. These two structural parameters (and possibly others), considered by the authors to be very important in the characterization of the solvation in mixed solvents, are also subject to strong dependence on the solute conformation. Steric shielding of the alcoholic group, different atomic charges for primary, secondary and tertiary carbons, 5−10% changes of the oxygen and alcoholic hydrogen charges in different solvents, all lead to solution structures where simple prediction of the hydrogen-bond pattern on the basis of the bulk dielectric constant is impossible. As a conclusion drawn from the present study, the solvents with at least 50% water content behave similarly to pure water in solvating secondary and tertiary alcohols. By similarity is meant the arrangement of the water molecules in the first solvent shell of the solute polar sites and a similar number of hydrogen bonds in pure water versus the mixture. Solvation of the primary alcohols is, however, more sensitive to the acetonitrile content in the mixture, and even in

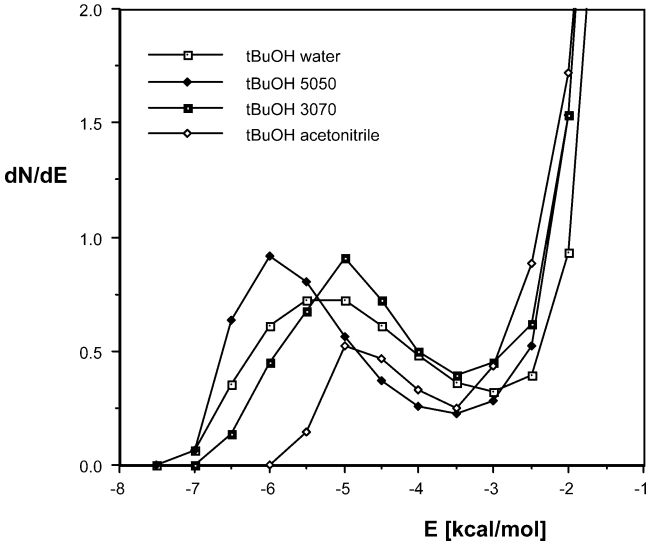

Figure 14. Pair-energy distribution functions for *t*-BuOH in pure solvents and mixtures.

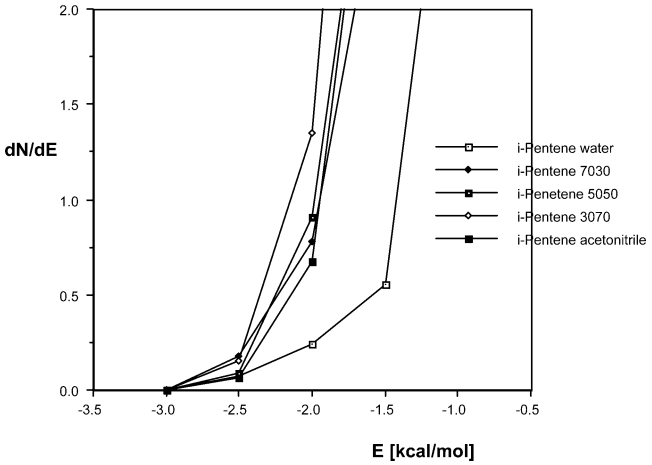

Figure 15. Pair-energy distribution functions for isopentene in pure solvents and mixtures.

w:acn = 70:30 mixtures the number of hydrogen bonds remarkably decreases. Increase of the acetonitrile fraction above 50% strongly reduces the number of hydrogen bonds for almost every solute/conformer. Nonetheless, even in solutions with only 10% water fraction, O−H···O_w hydrogen bonds are possible for a shorter or longer time (in a smaller or a larger fraction of snapshots studied; Figures 1 and 2).

With only pair interactions considered in the present study and many approximations applied in developing simulation parameters, the results should be taken to have only limited general relevance. As one reviewer noted, the solvation in mixed solvents is a complicated problem that might be reliably handled only in a QM/MM scheme, where the QM part contains the solute, first solvation shell, and one layer of bulk solvent. Such a calculation when implemented in Monte Carlo simulations (MC-QM/MM method[29]), however, would be extremely time-consuming for medium-size solutes even at the B3LYP/6-31G* level. Furthermore, while one may keep the composition (number of solvent molecules) constant for the QM system with a single solvent, a switch of the solvent molecules must be allowed for mixed solvents, and this will cause an even slower convergence in the system's total energy.

Figure 15 shows the pedfs for isopentene at different solvent compositions. The onset is at a slightly negative *E* value of −2.5 kcal/mol. The more important difference in comparison with pedfs in Figures 11−14 is, however, that the isopentene pedfs do not show the maximum−minimum course found to be characteristic for each alcohol in any studied solvent. The monotonic increase of the pedf means that there is not a (small) group of the solvent molecules in special, fairly strong interaction with the solute. The special interaction for alcohols was the hydrogen bond with donor and/or acceptor solvent molecules. The possible H_w···double-bond (H_w···π-electrons) interaction, discussed in the previous section, must be weak if it exists at all. The weakness of this interaction could be concluded from the absence of the maximum−minimum course of the pedf. Consequently, no upper integration limit exists for these curves, and no strongly bound solvent molecules can be identified in hydrogen-bond to the isopentene solute. This is entirely in accord with classical structure expectations.

Conclusions

The present status of development of the polarizable continuum dielectric method (PCM) does not provide an answer about how to handle the solvation of molecules having both polar and apolar sites in mixed solvents, particularly when the solvent components possess hydrogen-bond-forming capacity. We outline a direction for program development, wherein (1) a continuum dielectric method would accept more than one solvent; (2) solvation sites would be specified for the solute in one of its conformational and/or tautomeric states by the user; (3) the specified sites would, in turn, be solvated by user-defined solvent components; (4) the program would then set up the corresponding internal (dielectric, cavity size, dispersion, and repulsion) parameters and performs the PCM calculations; and (5) by changing the conformational/tautomeric states and/or the solvation pattern in a systematic way or investigating a particular arrangement of interest, the resulting free energy will be calculated so as to be available for comparison within the immediate data set as well as to any experimental data that may be available with regard to the nature of the solvation shell. In the absence of experimental data, the solute's structure and the solvation pattern providing the lowest free energy for the system can be considered as the prevailing solvation model of the given solute for the mixed solvent in question. Likewise, multiple systems having similarly low free energies can be considered to represent reasonably well-populated sets of interchanging arrangements. It is to be noted, however, that the present approach does not consider the free energy contribution due to the reorganization of the solvent components throughout the solvation.

The proposed development of such a program (or something better) is necessary because Monte Carlo studies for simple alcohols (ethyl, isobutyl, isopropyl, and *tert*-butyl) show that the solutes do indeed "discriminate" the solvent components and that the composition of the first solvation shell differs from that of bulk. Characterization of equilibrium hydrogen-bond formation is a complicated problem in mixed water−acetonitrile solutions that depends on the chemical properties of the solute and its conformation, as well as upon the varying nature of the first solvation shell. The present study suggests that a mixed water−acetonitrile solvent system having at least 50% water content behaves like pure water in terms of solvation and hydrogen-bond formation when the solute is a secondary or a tertiary alcohol. These alcohols tend to form two hydrogen bonds with solvent molecules in the indicated water fraction range. Alternatively, the number of hydrogen bonds with primary alcohol solutes appears to be more sensitive to the acetonitrile content. Although primary alcohols in some conformations form

2.4−2.7 hydrogen bonds in pure water, this value decreases to 1.4−2.0 in water:acetonitrile mixtures of 50:50. When acetonitrile begins to predominate, the number and the strength of the hydrogen bonds further decrease, and when acetonitrile is present at about 70% or more in the mixture, the solution structure becomes close to that in pure acetonitrile. Nonetheless, even in these solutions, O−H···O_w hydrogen bonds are possible in a small fraction of configurations. The isopentene solute, even with a C═C double bond to serve as an electron-rich site, did not form observable hydrogen bonds in our studies.

Acknowledgment. We are indebted to Professor Jorgensen for permission to use the BOSS 3.6 software and to the Ohio Supecomputer Center for computer time granted for the ab initio calculations. Useful discussions with Drs. Alagona and Ghio about the application of the PCM method are also appreciated.

References and Notes

(1) Hehre, W. J.; Radom, L.; Schleyer, P. v. R.; Pople, J. A. *Ab Initio Molecular Orbital Theory*; Wiley: New York, 1986.

(2) (a) Becke, A. D. *J. Chem. Phys.* **1993**, *98*, 5648. (b) Lee, C.; Yang, W.; Parr, R. G. *Phys. Rev. B* **1988**, *37*, 785.

(3) See, for example, (a) Böttcher, C. J. F. *Theory of electric polarisation*; Elsevier: Amsterdam, 1952. (b) Miertus, S.; Scrocco, E.; Tomasi, J. *Chem. Phys.* **1981**, *55*, 117. (c) Tomasi, J.; Persico, M. *Chem. Rev.* **1994**, *94*, 2027. (d) Angyan, J. *J. Math. Chem.* **1992**, *10*, 93. (e) Cramer, C. J.; Truhlar, D. G. *Chem. Rev.* **1999**, *99*, 2161. (f) Orozco, M.; Luque, F. J. *Chem. Rev.* **2000**, *100*, 4187.

(4) Jellema, R.; Bulthuis, J.; Van der Zwan, G. *J. Mol. Liquids* **1997**, *73*, *74*, 179.

(5) (a) Alagona, G.; Ghio, C.; Nagy, P. I. *Int. J. Quantum Chem.* **2004**, *99*, 161. (b) Nagy, P. I. *J. Phys. Chem. B* **2004**, *108*, 11105. (c) Nagy, P. I.; Takács-Novák, K. *Phys. Chem. Chem. Phys.* **2004**, *6*, 2838. (d) Nagy, P. I. *J. Phys. Chem. A* **2002**, *106*, 2659.

(6) (a) Zwanzig, R. W. *J. Chem. Phys.* **1952**, *22*, 1420. (b) Jorgensen, W. L.; Ravimohan, C. *J. Chem. Phys.* **1985**, *83*, 3050.

(7) (a) Nagy, P. I.; Dunn, W. J., III; Alagona, G.; Ghio, C. *J. Am. Chem. Soc.* **1991**, *113*, 1489. (b) Nagy, P. I.; Dunn, W. J., III; Alagona, G.; Ghio, C. *J. Am. Chem. Soc.* **1992**, *114*, 4752.

(8) (a) Kakar, R. K.; Quade, C. R. *J. Chem. Phys.* **1980**, *72*, 4300. (b) Michielsen-Effinger, J. *J. Mol. Spectrosc.* **1969**, *29*, 489. (c) Michielsen-Effinger, J. *J. Phys. (Paris)* **1969**, *30*, 336.

(9) Same as ref 1.

(10) McQuarrie, D. A. *Statistical Mechanics*; University Science Books: Sausalito, CA, 2000.

(11) . (a) Frisch, M. J.; Trucks, G. W.; Schlegel, H. B.; Scuseria, G. E.; Robb, M. A.; Cheeseman, J. R.; Zakrzewski, V. G.; Montgomery, J. A.; Stratmann, R. E.; Burant, J. C.; Dapprich, S.; Millam, J. M.; Daniels, A. D.; Kudin, K. N.; Strain, M. C.; Farkas, O.; Tomasi, J.; Barone, V.; Cossi, M.; Cammi, R.; Mennucci, B.; Pomelli, C.; Adamo, C.; Clifford, S.; Ochterski, J.; Petersson, G. A.; Ayala, P. Y.; Cui, Q.; Morokuma, K.; Malick, D. K.; Rabuck, A. D.; Raghavachari, K.; Foresman, J. B.; Cioslowski, J.; Ortiz, J. V.; Stefanov, B. B.; Liu, G.; Liashenko, A.; Piskorz, P.; Komaromi, I.; Gomperts, R.; Martin, R. L.; Fox, D. J.; Keith, T.; Al-Laham, M. A.; Peng, C. Y.; Nanayakkara, A.; Gonzalez, C.; Challacombe, M.; Gill, P. M. W.; Johnson, B. G.; Chen, W.; Wong, M. W.; Andres, J. L.; Head-Gordon, M.; Replogle, E. S.; Pople, J. A. Gaussian 98 (Revision A.6); Gaussian, Inc.: Pittsburgh, PA, 1998. (b) Gaussian 03 User's Reference, http://www.Gaussian.com/g_ur/k_scrf.htm.

(12) *CRC Handbook of Chemistry and Physics*, 85th ed.; Lide, D. R., Ed.; CRC Press: Boca Raton, FL, 2004.

(13) Breneman, C. M.; Wiberg, K. B. *J. Comput. Chem.* **1990**, *11*, 316.

(14) (a) Jorgensen, W. L.; Madura, J. D. *J. Am. Chem. Soc.* **1983**, *105*, 1407. (b) Jorgensen, W. L.; Swenson, C. J. *J. Am. Chem. Soc.* **1985**, *107*, 1489. (c) Jorgensen, W. L.; Gao, J. *J. Phys. Chem.* **1986**, *90*, 2174. (d) Jorgensen, W. L.; Briggs, J. M.; Contreras, M. L. *J. Phys. Chem.* **1990**, *94*, 1683.

(15) (a) Jorgensen, W. L. BOSS, Version 3.6, *Biochemical and Organic Simulation System User's Manual*; Department of Chemistry, Yale University: New Haven, CT, 1995. (b) Metropolis, N.; Rosenbluth, A. W.; Rosenbluth, M. N.; Teller, A. H.; Teller, E. *J. Chem. Phys.* **1953**, *21*, 1087.

(16) Jorgensen, W. L.; Chandrasekhar, J.; Madura, J. D.; Impey, R. W.; Klein, M. L. *J. Chem. Phys.* **1983**, *79*, 926.

(17) Jorgensen, W. L.; Briggs, J. M. *Mol. Phys.* **1988**, *63*, 547.

(18) (a) Jorgensen, W. L.; Maxwell, D. S.; Tirado-Rives, J. *J. Am. Chem. Soc.* **1996**, *118*, 11225. (b) Rizzo, R. C.; Jorgensen, W. L. *J. Am. Chem. Soc.* **1999**, *121*, 4827.

(19) Lees, R. M.; Baker, J. G. *J. Chem. Phys.* **1968**, *48*, 5299.

(20) (a) Nagy, P. I.; Dunn, W. J., III; Alagona, G.; Ghio, C. *J. Phys. Chem.* **1993**, *97*, 4628. (b) Nagy, P. I.; Alagona, G.; Ghio, C.; Takács-Novák, K. *J. Am. Chem. Soc.* **2003**, *125*, 2770.

(21) For C−H···O hydrogen bonds see, for example, (a) Gu, Y.; Kar, T.; Scheiner, S. *J. Am. Chem. Soc.* **1999**, *121*, 9411. (b) Hobza, P.; Havlas, Z. *Chem. Rev.* **2000**, *100*, 4253. (c) Scheiner, S.; Kar, T. *J. Phys. Chem. A* **2002**, *106*, 1784. (d) Li, X.; Liu, L.; Schlegel, H. B. *J. Am. Chem. Soc.* **2002**, *124*, 9639.

(22) (a) Suzuki, S.; Green, P. G.; Bumgarner, R. E.; Dasgupta, S.; Goddard, W. A., III; Blake, G. A. *Science* **1992**, *257*, 942. (b) Augspurger, J. D.; Dykstra, C. E.; Zwier, T. S. *J. Phys. Chem.* **1993**, *97*, 980.

(23) Tarakeshwar, P.; Choi, H. S.; Lee, S. J.; Lee, J. Y.; Kim, K. S.; Ha, T. K.; Jang, J. H. Lee, J. G.; Lee, H. *J. Chem. Phys.* **1999**, *111*, 5838.

(24) Kovacs, H.; Laaksonen, A. *J. Am. Chem. Soc.* **1991**, *113*, 5596.

(25) Nakanishi, K.; Ikari, K.; Okazaki, S.; Touhara, H. *J. Chem. Phys.* **1984**, *80*, 1656.

(26) Tanaka, H.; Nakanishi, K.; Touhara, H. *J. Chem. Phys.* **1984**, *81*, 4065.

(27) (a) Noto, R.; Martorana, V.; Emanuele, A.; Fornili, S. L. *J. Chem. Soc., Faraday Trans.* **1995**, *91*, 3803. (b) Bowron, D. T.; Finney, J. L.; Soper, A. K. *Mol. Phys.* **1998**, *93*, 531. (c) Kusalik, P. G.; Lyubartsev, A. P.; Bergman, D. L.; Laaksonen, A. *J. Phys. Chem. B* **1999**, *104*, 9533.

(28) Cramer, C. J. *Essentials of Computational Chemistry*; Wiley: New York, 2002; pp 78−80.

(29) (a) Field, M. J.; Bash, P. A.; Karplus, M. *J. Comput. Chem.* **1990**, *11*, 700. (b) Luzhkov, V.; Warshel, A. *J. Comput. Chem.* **1992**, *13*, 199. (c) Gao, J. *J. Phys. Chem.* **1992**, *96*, 537. (d) Gao, J.; Xia, X. *Science* **1992**, *258*, 631. (e) Gao, J.; Luque, F. J.; Orozco, M. *J. Chem. Phys.* **1993**, *98*, 2975.